Chapter 1- Introduction

1.1 Introduction

Rigid-frame construction may require a slightly greater amount of steel than a truss-column frame, but the simplicity and speed of erection result in appreciable savings. The use of welding and plastic design may achieve further advantageous. By means of elastic design it is possible to analyse several combinations of independent loading of the structure, elasticity has the advantage that the superposition rules are applicable. However, the rules of superposition are not valid in plastic design. The location of plastic hinges in a frame varies with the type of loading, shape and physical properties of the frame. To determine the location and minimum number of plastic hinges needed for mechanism with the given loading, various analytical procedures may be applied to frames. The most widely used is the energy and equilibrium method. If plastic deformation takes place forces and moments can be determined by using methods of equilibrium. When full plastification occurs at certain critical sections of a frame, it leads to the development of plastic hinges. The ultimate load is usually defined as the load which produces a sufficient number of plastic hinges to convert the structure into a mechanism. To estimate limit loads is the aim of several papers, for example, J. Shi, D. Mackenzie, and J.T.Boyle (1993) developed a method of estimating limit loads by iterative elastic analysis.

The adoption of limit states concepts in design practice has made it mandatory for engineers to evaluate the load carrying capacities of structures. This task commonly referred as limit analysis, is concerned with the strength of ductile structure and not with deformation. Limit state solutions have been given by A.R.S. Ponter and K.F. Carter (1995). These solutions are based upon linear elastic solutions with a spatially varying elastic modulus. It involves the determination of the maximum load amplification or safety factor for a perfectly plastic structure subject to proportional loading. Plastic collapse occurs when the structure is converted into a mechanism by provision of a suitable number of disposition of plastic zones.

For standard materials, the plastic limit analysis problem can be solved trough application of either of a pair of dual theorems. These notions, referred to as the static (safe or lower bound) theorem and the kinematic (unsafe or upper bound) theorem, were developed in the early 1950s and are strongly suggestive of a constrained optimisation approach. In practice, however, the analysis is rarely carried out as such, engineers tend to adopt a manual trial mechanism approach which is cumbersome to use except for the simplest cases of discrete structures for which plasticity is governed by a single stress resultant. Surprisingly some analysts still resort to step-by step calculations, no doubt because of their accumulated experience with traditional linear elastic analyses.

When distributed loads are considered or when other contributions rather than pure plastic bending are considered, a manual calculation is not possible. We have to use numerical algorithms. In this paper we use algorithms based on the error estimation. M. Ainsworth and J.T.Oden (2000) and P. Ladaveze and D. Leguillon (1983) are papers that introduce error estimation algorithms. The application of mathematical

programming concepts for encoding the behaviour of discrete plastic structural systems is a well developed area. Vigorous research, article J.Bonet, A. Huerta and J. Peraire (2002), over the last two decades has produced a unified theoretical frame work for the study of such systems. Graph theoretic network aspects have also been systematically exploited within this broad field. Moreover, in addition to its use as a conceptual tool, with its collection of well constructed algorithms, often offers a clear and efficient means of obtaining numerical solutions to a wide range of plasticity problems, including limit analysis.

The primary aim of this work is to find a sequence of upper and lower bounds of the real collapse load of a frame structure. A perfect plastic model is used. A.R.S. Ponter, Paolo Fuschi and Markus Engelhardt (2000) develop an analysis for general class of yield conditions. It is taken into account the contribution of plastic bending and tension (or compression). Other effects are not considered. Besides, a program in Fortran has been elaborated to obtain the upper and lower bounds. The process starts with an initial mesh of the structure. Then, this mesh is refined until convergence of the upper and lower bounds. The refinement process is based on the evaluation of the gap between the lower and upper bounds. In order to optimise the mesh, this is to consider the fewer elements, we can manipulate a parameter that allow us to decide whether one element contributes enough or it does not.

In order to solve the limit analysis problem, the method we have implemented is based on the evaluation of a secant matrix. This secant matrix is obtained directly from the optimisation problem.

This work is the continuation of a thesis developed by McCulloch (2002). This thesis focuses on the limit analysis of trusses and beams. This work has been extended by adding axial affects. Also we have extended the analysis to frames. The application of the limit analysis theorems does not ends in frames. There has been a large research for shells. For example A.R.S. Ponter and S. Karadeniz (1980) or K.F.Carter and A.R.S. Ponter (1990). Finally, we have implemented all the theory explained in this work in a program. This program uses subroutines of the program Lingflag, developed by Javier Bonet.

1.2 Applicability of the method

This work is based on the following assumptions

- Displacements are small so that the equilibrium equations refer to the initial, undeformed structure geometry.

- Perfect rigid plasticity.

- The structure collapses because a plastic limit state. Other ways of collapsing are neglected. We point out this fact, because we have to combine the method we propose with a study of the stability of the structure in order to know if the structure collapses before it reaches the plastic limit state. Z.Waszczyszyn (1994) developed methods to study the stability using finite element methods. Although an analysis of stability is necessary, we it is not the aim of this work.

- Proportional loading. We consider that all the loads depend on one parameter called plastic multiplier. Therefore, the loads are dependent. We do not consider independent loads.

- Plastic deformations are consistent with the normality rule of the classical theory of plasticity.

- The structure is plane and consists of straight prismatic elements interconnected at nodes.

- The sign of the stress coincides with the sign of the strain. This hypothesis is valid when the loading process is monotonic.

Chapter 2. Plastic analysis of structures under uniaxial stress – Fundamentals

This chapter is a review of the most important concepts of plasticity of structures under unaxial stress. It has been introduced to make this paper understandable to a larger number of readers. Most of the explanations given in the following lines have been taken from the book Milan J., Zdenek P. (2001).

2.1 Uniaxial Stress-Strain Relations

Before focusing on the specific problem this thesis is based on, it is important to brush up some of the elementary aspects of plasticity. The stress-strain diagram of different metals is shown in Figure 2.1. As The strain is increased, the stress first increases linearly until a certain critical value, the *elasticity limit*, is reached. At that point the behavior of the metal changes completely. This second step varies from metal to metal. For example, the diagram of mild steel continues with a small and abrupt 'hump', a transition to a horizontal plateau characterized by a stress value σ_o called the yield stress, as shown in Figure 2.1(a).

For other metals their behavior after the elastic zone is different. For example, alloy steels do not have a defined yield plateau. In this case It is found a smooth decline of the slope of the uniaxial stress-strain diagram, as shown in Figure 2.1(b).

All this different behaviors can be modeled, for the purpose of a more simple structural analysis, by idealized stress-strain diagrams. Figure 2.1(c) shows the *elastic-perfectly plastic* behavior. In this diagram the stress σ cannot exceed the bounds given by the yield stress in tension, σ_y^+, and de yield stress in compression, $-\sigma_y^-$. Any value of stress that satisfies this condition is called *plastically admissible*. For metals, both yield stresses usually have the same magnitude, $\sigma_y^+ = \sigma_y^- = \sigma_y$. The condition of *plastic admissibility then reads*

$$-\sigma_y \leq \sigma \leq \sigma_y \tag{2.1}$$

Therefore, plastic yielding can take place only if

$$|\sigma| - \sigma_y = 0 \tag{2.2}$$

It is important to note that the expression (2.1) in its strict form defines the *elastic domain*. When the plastic deformations are many times larger than the elastic limit, we can simplify even more the stress-strain diagram. Then we have a *rigid-perfectly plastic* behavior, as shown in figure 2.1(d). The elastic branch has been eliminated. Practice has shown us that this simplified diagram is really useful when working out collapse loads. The reason is that during collapse, the critical cross sections are at strains much larger than the elastic ones.

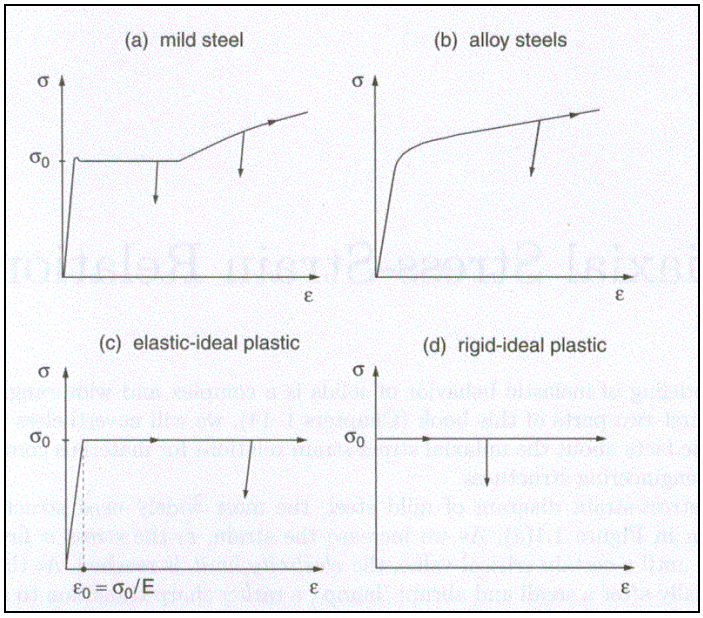

Figure 2.1 Uniaxial stress-strain diagrams.

Before starting to solve a structure, you have to know the real behavior of the materials used in the structure, and the possible simplifications that can be done in order to simplify the calculus. In this thesis we deal with materials that can be modeled by the *rigid-perfectly plastic* diagram. Therefore the method of calculus developed in this work makes the assumption that the material has a *rigid-perfectly plastic* behavior.

There are many other types of behavior that cannot be modeled by the *rigid-perfectly plastic* behavior. Figure 2.2 shows some of these uniaxial stress-strain diagrams.

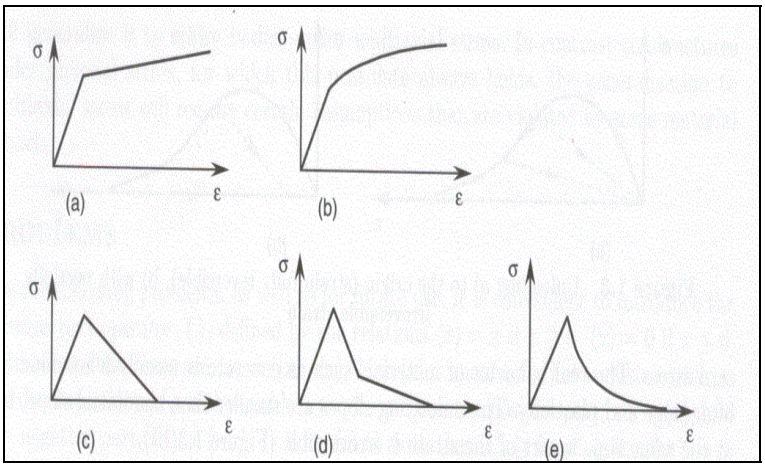

Figure 2.2 Uniaxial stress-strain diagrams: a) linear hardening, b) nonlinear hardening, c) linear softening, d)bilinear softening, e)exponential softening.

Let's focus now on the strain. The main property for which the behavior of a material is called plastic is the *irreversibility of deformation* upon loading. For ductile materials such as metals, in which the inelastic deformation is mainly due to slip in the microstructure, the slopes of the stress-strain diagram for unloading are essentially the same as the initial (elastic) slope. In the context of small-strain theory, this leads to the additive decomposition

$$\varepsilon = \varepsilon_e + \varepsilon_p \tag{2.3}$$

Where

ε is the total strain
ε_e is the elastic strain
ε_p is the plastic strain

During elastic loading (or unloading), the mechanical work done on the material is converted to the store elastic energy. During plastic yielding, a part of this work is dissipated by irreversible plastic processes in the material, usually as heat.

For perfect elastoplastic materials, the *rate of dissipation per unit volume* is given by the product of the stress and the plastic strain rate. The stress during plastic yielding is either $\sigma = \sigma_y$, and then the plastic strain rate must be positive, or $\sigma = -\sigma_y$, and then the plastic strain rate must be negative. In either case, the elastic strain remains constant. Consequently, the dissipation per unit volume is

$$\hat{D}_{\text{int}} = \sigma \dot{\varepsilon} = \sigma_y \mid \dot{\varepsilon} \mid \tag{2.4}$$

and $\dot{\varepsilon}$ is the plastic strain rate.

Therefore, the dissipation per unit volume depends only on the plastic strain rate. Now, suppose that, at a given point, the material yields under uniaxial stress. Let σ_s be any plastically admissible stress. This stress satisfies condition (2.1), then

$$\sigma_s \dot{\varepsilon}_p \leq \mid \sigma_s \mid\mid \dot{\varepsilon}_p \mid \leq \sigma_y \mid \dot{\varepsilon}_p \mid = D_{\text{int}}(\dot{\varepsilon}_p) \tag{2.5}$$

Consequently, the actual stress σ needed to induce a given plastic strain rate maximizes the product the plastically admissible stress σ_s and the plastic rate, among all the values of σ_s:

$$\hat{D}_{\text{int}}(\dot{\varepsilon}_p) = \sigma \dot{\varepsilon}_p = \max_{\sigma_s \in \xi}(\sigma_s \dot{\varepsilon}_p) \tag{2.6}$$

where

$\xi = [-\sigma_y, \sigma_y]$ is the set of plastic admissible stress states.

Statement (2.6) is a special case of the postulate of maximum plastic dissipation. We will use this postulate to prove the principal theorems of Limit Analysis.

2.2 Plastic Bars and Yield Hinges

In this section the concepts of Plastic Moment and plastic Hinge are introduced. These concepts will be useful in order to reach a better understanding of the plastic behavior of a beam.

2.2.1 Plastic Moment

The first case that is solved is the collapse load for a continuous beam under loads perpendicular to its longitudinal axis. This means that the beam will collapse under bending. If it is assumed that the plane cross sections remain plane, and that they remain normal to the deflected middle axis of the beam. Then, the relation between the bending moment and the curvature of the deformed middle axis can be found. These assumptions are valid for elastic as well as inelastic bending, provided the beam is sufficiently long compared to its cross section dimensions (for good accuracy, at least ten times longer). In this case the strain can be expressed as follows,

$$\varepsilon = zk \tag{2.7}$$

in which z is the depth coordinate measured form the middle axis, and k is the curvature. Figure 2.1 shows a rectangular cross section under pure bending.

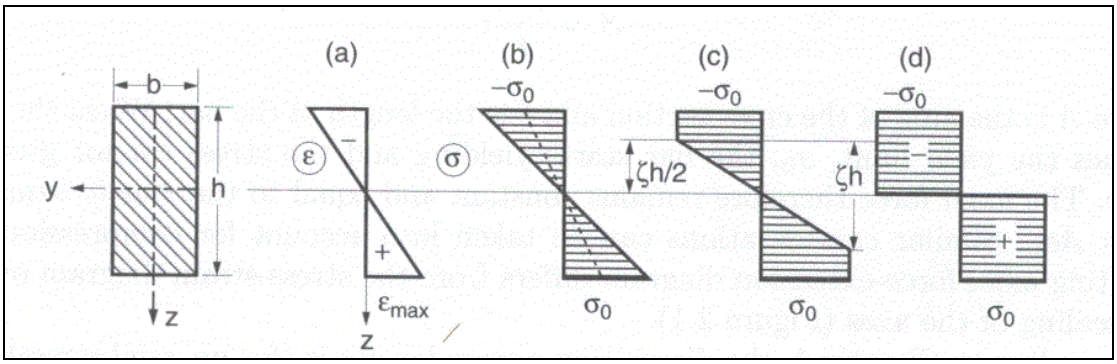

Figure 2.3 Rectangular cross section under pure bending: a) strain distribution, b) stress at the elastic limit state, c) stress at an elastoplastic state, d) stress at the plastic limit state.

The bending moment when the cross section is at the plastic limit state is

$$M_p = \int_A \sigma_y z dA \tag{2.8}$$

For a rectangular cross section with width b and height h the plastic moment is therefore,

$$M_p = \sigma_y \frac{bh}{4} \tag{2.9}$$

These expressions will be used later in order to work out the plastic dissipation rate.

2.2.2 Plastic Hinge

In this section it is assumed that the effect of normal and shear forces on the formation of the plastic hinge is negligible, and that a plastic hinge forms when the bending moment reaches the plastic limit moment of the cross section.

When studying the behavior of a beam at collapse state it is observed that the real plasticized zone occupies a certain volume. This volume is concentrated around

completely plasticized cross sections. For structural purposes we will suppose that all the plastic deformation of a plasticized zone can be lumped into a single cross section with infinite curvature surrounded by elastic material. This cross section is equivalent of a hinge. We call it *plastic hinge*. Beams and Frames fail after a sufficient number of plastic hinges form in the most exposed cross sections and the structure turns into a mechanism.

It is important to note that the concept of plastic hinge does not require the plastic rotation to be large. During collapse the load is constant, therefore the elastic deformations do not change. This means that all the structural parts whose cross section is not fully plasticized behave as a rigid body. This implication has consequences in the way the structural problem will be solved. In essence, the problem will be reduced to the solution of a nonelinear system with a badly conditioned matrix. All the plastic deformation is concentrated into few cross sections. Therefore, considering a mesh that represents the structure, most of the elements have no plastic deformation. They act as rigid bodies, which means that their contribution to the final assembled matrix tends to infinity, and so the difference between the bigger and the smaller eigenvalue is very large.

The plastic hinge means that the total plastic deformation can be replaced by a rotation, θ, in an idealized hinge (Figure 2.4).

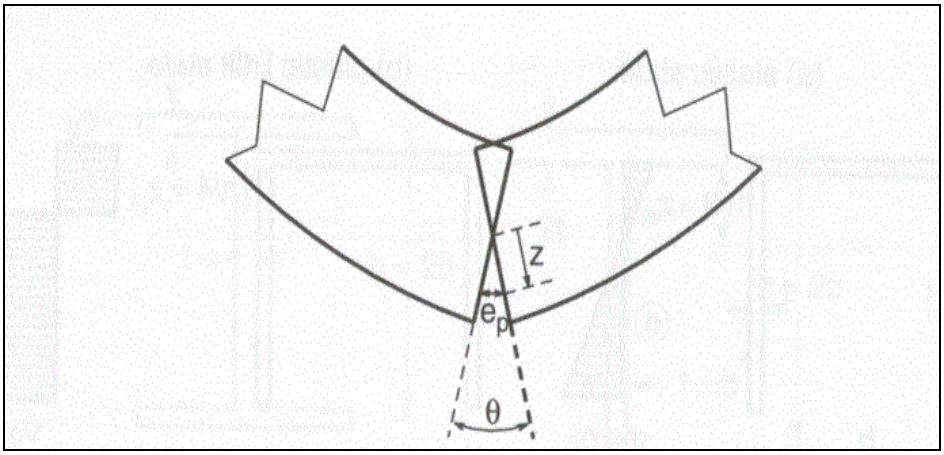

Figure 2.4 Idealized plastic hinge.

From kinematic considerations, it follows that the plastic extension at an arbitrary point of the cross section can be expressed by a linear function

$$e_p(z) = \theta \cdot z \tag{2.10}$$

from this expression, it can be worked out the power dissipated by a plastic hinge

$$D_{\text{int}} = \int_V \sigma \dot{\varepsilon}_p \, dV \tag{2.11}$$

The definition of the plastic hinge allows us to express (2.11) by the integral over the fully plasticized cross section

$$D_{\text{int}} = \int_A \sigma(z)\dot{e}_p(z)dA \tag{2.12}$$

because the extension $e_p(z)$ corresponds to the plastic strain at z integrated over the length of the plastic hinge. Substituting expression (2.10) for the plastic extension, equation (2.12) becomes,

$$D_{\text{int}} = \int_A \sigma(z)\dot{\theta}\, z dA = \int_A \sigma(z) z dA\, \dot{\theta} = M\dot{\theta} \tag{2.13}$$

Now, by analogy with (2.4), the dissipation power in a plastic hinge can be expressed as

$$D_{\text{int}} = M\dot{\theta} = M_p |\dot{\theta}| \tag{2.14}$$

Let's introduce the main theorems of the limit state analysis.

2.3 Limit analysis

2.3.1 Introduction

The aim of the limit analysis is to work out the collapse load of a certain structure without analyzing the entire history of the response. In general, any structure must become a kinematic mechanism for plastic collapse to occur. Limit analysis allows us to find the mechanism at collapse state. There has been a large research in limit analysis. Milan Jirasek and Zdenek P. Bazant (2001) have proposed methods based on limit analysis where the optimization problems are solved using linear optimization. Other papers concentrate on the evaluation of bounds by elastic finite element analysis D. Mackenzie, C. Nadarajah, J. Shi and J.T. Boyle (1993).

During collapse, the external loads remain constant, and they do some work on the increasing displacements. The product of the forces and the displacement rates defines the external power as,

$$\dot{W}_{ext} = \int_v \mathbf{b}^T \dot{\mathbf{v}}\, dV + \int_{\partial V} \mathbf{t}^T \dot{\mathbf{v}}\, dS + \sum_i^n \mathbf{F}_i^T \dot{\mathbf{v}}_i \tag{2.15}$$

where **b** are the volume loads, **t** the distribute surface loads and **F** the point loads.

This power is supplied to the structure and, assuming a steady-state collapse with no inertial effects, it must be dissipated by processes in the yielding bars. We can express this fact as the *power equality*

$$\dot{W}_{ext} = D_{\text{int}} \tag{2.16}$$

This is the equilibrium equation that the limit analysis is based on.

2.3.2 Theorems of Limit Analysis

At this point, the basic concepts of limit analysis will be introduced.

Plastic limit load multiplier

Consider proportional loading described by the load multiplier μ . The multiplier for which the structure collapses is called the *plastic limit load multiplier* and is denoted by μ_o.

Statically admissible state

A *statically admissible state* of a structure is any plastically admissible stress field that is in equilibrium with a certain multiple of the reference loading and that satisfies the yield conditions. The corresponding load multiplier μ_s is called a *statically admissible load multiplier*.

Kinematically admissible state

A *kinematically admissible state* is defined as any potential failure mechanism for which the external power is positive. The corresponding load multiplier μ_k, determined from the power equality, is called the *kinematically admissible multiplier*.

Considering a discretisation, the external power can be expressed as a product of a load vector $\mathbf{f}^T$ and a nodal displacements vector $\dot{\mathbf{v}}$. And using the kinematically admissible multiplier, the external power can be expressed as,

$$\dot{W}_{ext} = \mathbf{f}^T \dot{\mathbf{v}} = \mu_k \hat{\mathbf{f}}^T \dot{\mathbf{v}} \tag{2.17}$$

Now, the value of μ_k can be obtained by using the equation (2.16)

$$\mu_k = \frac{D_{\text{int}}}{\hat{\mathbf{f}}^T \dot{\mathbf{v}}} \tag{2.18}$$

Postulate of Maximum Plastic Dissipation

For given generalized plastic strain rates, the actual internal forces maximize the plastic dissipation rate among all the plastically admissible internal forces.

This postulate is valid in either beam and frame structures considering either only bending or the combination of bending and stress.

Fundamental Theorem of Limit Analysis

No statically admissible multiplier is larger than any kinematically admissible multiplier.

Upper Bound Theorem

If there is a potential failure mechanism for which the dissipation rate is smaller than the external power supplied by the given loads, the structure will collapse under such loads.

Lower Bound Theorem

If there is a state of stress that is inside the elastic domain and is in equilibrium with the given applied loads, the structure will not collapse under such loads.

Chapter 3. Plastic Limit Analysis

The aim of this chapter is to introduce a method based on the limit analysis theory and the Finite Element theory, that allow us to obtain upper and lower bounds of a *plane stress* 2-d solid. The difference between these upper and lower bounds defines the gap which will be expressed as sum of positive element contributions. In future chapters this method will be applied to more simple cases: beams and frames.

3.1 Plastic Potential

Consider a simple Von-Mises material. The rate of plastic dissipation for a given rate of deformation tensor **d** is given as,

$$D_{\text{int}}(\mathbf{d}) = \sigma_y \, \dot{\bar{\varepsilon}}(\mathbf{d}) \tag{3.1}$$

$$\mathbf{d} = \frac{1}{2}(\nabla \mathbf{v} + \nabla \mathbf{v}^T) \tag{3.2}$$

Where **v** is the displacement vector, σ_y is the yield stress and $\dot{\bar{\varepsilon}}(\mathbf{d})$ the equivalent strain rate given by Lubliner (1990)

$$\dot{\bar{\varepsilon}} = \sqrt{\frac{2}{3}(\mathbf{d}' : \mathbf{d}')} \tag{3.3}$$

is a function of the deviator of the deformation tensor $\mathbf{d}'$. Note that,

$$D_{\text{int}}(\mathbf{d}) = \boldsymbol{\sigma} : \mathbf{d} \tag{3.4}$$

Note that the convexity of the yield surface and the normality rule for the plastic flow imply that

$$D_{\text{int}}(\mathbf{d}) \geq \boldsymbol{\sigma}^* : \mathbf{d} \tag{3.5}$$

for any $\boldsymbol{\sigma}^*$ inside the yield surface. The postulate of maximum plastic dissipation is obtained.

$$D_{\text{int}}(\mathbf{d}) = \max_{\boldsymbol{\sigma}^* \in P} \boldsymbol{\sigma}^* : \mathbf{d} \tag{3.6}$$

where P is space of stresses that satisfy yield criteria.

3.2 Upper Bound Theorem

Consider a 2-D (plane stress) body occupying an area A (Figure 3.1) with boundary $\Gamma = \partial A = \Gamma_f \cup \Gamma_u$. Γ_f is the part of the boundary under the action of surface forces loads, and Γ_u is the part of the boundary under the action of fixity conditions.

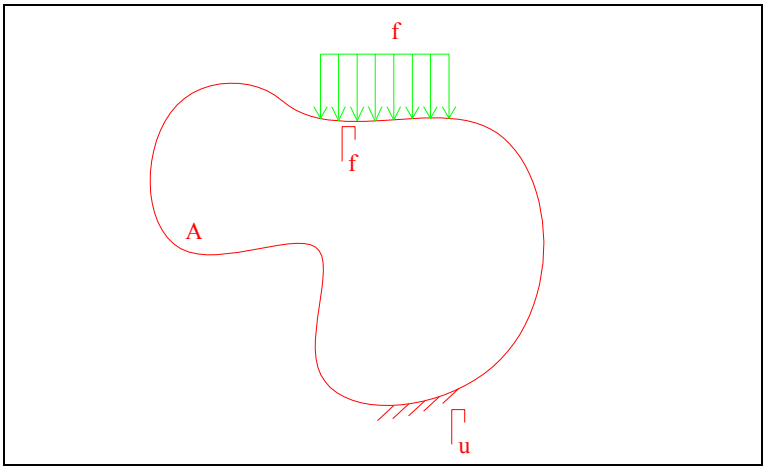

Figure 3.1 Load and boundary conditions

Assuming that the body is rigid-plastic with plastic potential $D_{\text{int}}(\mathbf{d})$, plastic flow will be initiated for a collapse multiplier μ_c and will lead to stresses $\boldsymbol{\sigma}_c$ in the body.

Equilibrium at this collapse state implies

$$\mu_c \int_{\Gamma_f} \hat{\mathbf{f}}^T \, \mathbf{v} ds = \int_A \boldsymbol{\sigma}_c : \mathbf{d} \; dA \qquad \forall \; \mathbf{v} \in X \tag{3.7}$$

X is the space of motions compatible with boundary conditions.

The work done by the external forces will be denoted by

$$W_{ext} = \int_v \mathbf{b}^T \, \mathbf{v} \, dV + \int_{\partial V} \mathbf{t}^T \, \mathbf{v} \, dS + \sum_i^n \mathbf{F}^T{}_i \, \mathbf{v}_i \tag{3.8}$$

The principle of maximum plastic dissipation implies

$$\boldsymbol{\sigma}_c : \mathbf{d} \le D_{\text{int}}(\mathbf{d}) \tag{3.9}$$

consequently

$$\mu_c W_{ext} \le \int_A D_{\text{int}}(\mathbf{d}) dA = D_{\text{int}} \tag{3.10}$$

the following inequality, known as the Upper Bound Theorem, is obtained

$$\mu_c \le \mu_{UB} \equiv \frac{D_{\text{int}}(\mathbf{v})}{W_{ext}(\mathbf{v})} \qquad \forall \; \mathbf{v} \in X \tag{3.11}$$

In particular, the collapse mechanism **u** is

$$\mu_c = \frac{D_{\text{int}}(\mathbf{u})}{W_{ext}(\mathbf{u})} = \min_{\mathbf{v}\in X} \frac{D_{\text{int}}(\mathbf{v})}{W_{ext}(\mathbf{v})} \tag{3.12}$$

Note, however, that both D_{int} and W_{ext} are homogeneous of order, that is $D_{int}(\alpha\mathbf{v}) = \alpha D_{int}(\mathbf{v})$; $W_{ext}(\alpha\mathbf{v}) = \alpha W_{ext}(\mathbf{v})$. Hence $\mathbf{u}$ is defined in direction but not in magnitude by (3.12). To remove this indetermination , the reduced space $\underline{X}$ is defined as

$$\underline{X} = \{\mathbf{v} \in X \mid W_{ext}(\mathbf{v}) = 1\} \tag{3.13}$$

and therefore

$$\mu_c = \min_{\mathbf{v}\in\underline{X}} D_{\text{int}}(\mathbf{v}) \tag{3.14}$$

Equation (3.14) gives us an easier way to find the upper bound. In conclusion, the problem that we face is a problem of optimization.

3.3 Finite Element Solution

Consider a mesh of the body and let X_H denote the corresponding solution space

$$X_H = \left\{ \mathbf{v} \in X \mid \mathbf{v} = \sum_{a=1}^{n} v_a N_a \right\} \tag{3.15}$$

For a given set of finite element shape functions N_a over a mesh with n nodes, consider also the reduced space $\underline{X}_H$

$$\underline{X}_H = \{\mathbf{v} \in X_H \mid W_{ext}(\mathbf{v}) = 1\} \tag{3.16}$$

The minimization is now

$$\mu_H = D_{\text{int}}(\mathbf{u}) = \min_{\mathbf{v}\in\underline{X}_H} D_{\text{int}}(\mathbf{v}) \tag{3.17}$$

Given that $\underline{X}_H \subset \underline{X}$, an upper bound of the solution is found

$$\mu_c \le \mu_H \tag{3.18}$$

In summary, the problem that will be solved to find an upper bound of the solution is the constrained minimization problem expressed by equations (3.16) and (3.14).

3.4 Lower Bound Evaluation

Consider a very fine mesh X_h obtained by enriching X_H by a higher order polynomials or element subdivision, X_h will be known as *reference mesh*. By construction $X_H \subset X_h$ and we will assume that the solution in X_h is sufficiently accurate, that is

$$\mu_c \approx \mu_h \equiv D_{\text{int}}(\mathbf{u_h}) = \min_{\mathbf{v}\in\underline{X}_h} D_{\text{int}}(\mathbf{v}) \tag{3.19}$$

where μ_c is very accurate to the real collapse load and the reduced space $\underline{X}_h$ is as before

$$\underline{X}_h = \{\mathbf{v} \in X_h \mid W_{ext}(\mathbf{v}) = 1\} \tag{3.20}$$

It is very important to note that the reference mesh has to be fine enough to achieve accurate results must be supposed. You have to note that solving the problem using the reference mesh would be impractical. Too many elements that do not contribute to the evaluation of the collapse load would be considered.

Now we will work out a lower bound of the approximation μ_c. Consider as the broken space $\hat{X}_h$ shown in figure (3.2), where continuity across the edges of X_H macroelements is not enforced.

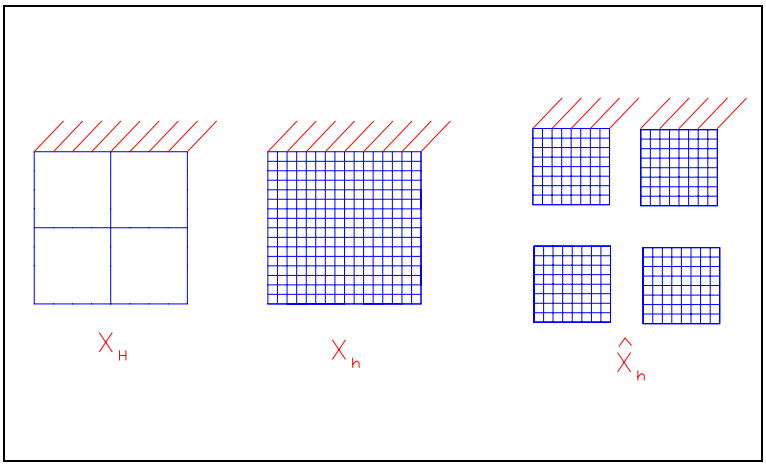

Figure 3.2 Different spaces of the body of study

Note that $X_h \subset \hat{X}_h$. To restore continuity, the edge forces **q** are introduced, such that

$$b(\mathbf{q}, \mathbf{v}) = \int_{\Gamma_f} \mathbf{q}[\mathbf{v}]ds \tag{3.21}$$

where [**v**] denotes the jump of **v** across the internal edges Γ_i. Then

$$X_h = \{\mathbf{v} \in \hat{X}_h \mid b(\mathbf{q}, \mathbf{v}) = 0 \ \ \forall \mathbf{q}\} \tag{3.22}$$

the reduced space $\underline{X}_h$ is now

$$\underline{X}_h = \{\mathbf{v} \in \hat{X}_h \mid W_{ext}(\mathbf{v}) + b(\mathbf{q}, \mathbf{v}) = 1 \ \ \forall \mathbf{q}\} \tag{3.23}$$

Note that the condition $W_{ext}(\mathbf{v})=1$ is obtained taking $\mathbf{q} = 0$. Expression (3.19) is now rewritten with the help of the Lagrangian as

$$\alpha_h(\mathbf{v}, \mathbf{q}, \gamma) = D_{\text{int}}(\mathbf{v}) + \gamma[1 - W_{ext}(\mathbf{v}) - b(\mathbf{q}, \mathbf{v})] \tag{3.24}$$

as

$$\mu_h = \min_{\mathbf{v}\in\hat{X}_h} \max_{\gamma,\mathbf{q}} \alpha(\mathbf{v},\mathbf{q},\gamma) \tag{3.25}$$

Duality now gives

$$\mu_h \geq \max_{\mathbf{q}} \min_{\mathbf{v}\in\hat{X}_h} \max_{\gamma} \alpha(\mathbf{v},\mathbf{q},\gamma) \tag{3.26}$$

$$\mu_h \geq \min_{\mathbf{v}\in\hat{X}_h} \max_{\gamma} \alpha(\mathbf{v},\mathbf{p_H},\gamma) \equiv \hat{\mu}_h \tag{3.27}$$

and therefore $\hat{\mu}_h$ is a lower bound of the approximation of the collapse load μ_c.

The term $\mathbf{p_H}$ in (3.27) represents a particular choice of $\mathbf{q}$ to be evaluated in the course mesh below. A simple expression for $\hat{\mu}_h$ is obtained by first defining the augmented external force term

$$\hat{W}_{ext} = W_{ext}(\mathbf{v}) + b(\mathbf{p_H},\mathbf{v}) \tag{3.28}$$

and the reduced broken space $\underline{\hat{X}}_h$ as

$$\underline{\hat{X}}_h = \left\{\mathbf{v}\in\hat{X} \mid \hat{W}_{ext}(\mathbf{v}) = 1\right\} \tag{3.29}$$

hence, $\hat{\mu}_h$ is now

$$\hat{\mu}_h \equiv D_{\text{int}}(\hat{\mathbf{u}}_\mathbf{h}) = \min_{\mathbf{v}\in\underline{\hat{X}}} D_{\text{int}}(\mathbf{v}) \tag{3.30}$$

The term $\mathbf{p_H}$ satisfies the following conditions,

- $\mathbf{p_H}$ must be continuous between the elements

- $\mathbf{p_H}$ in each broken space must be in equilibrium

When we are dealing with 2D elements, to warranty the equilibrium is not trivial. There has been a large research in this topic. For more detail you can find out in M. Ainsworth, J.T. Oden (2000) and P. Ladeveze, D. Leguillon (1983). For the case of a frame structure the equilibrium in the element is easy to obtain.

Despite the fact that condition (3.29) seems to tie up the solution of the local problems, they can in fact be solved individually. To show this consider each macroelement e=1,..,m_H in turn, where m_H is the number of elements in the coarse mesh. Consider the corresponding reduce space $\underline{Z}_h^e$

$$\underline{Z}_h^e = \left\{ \mathbf{v}^e \in Z_h^e \mid \hat{W}_{ext}^e(\mathbf{v}^e) = 1 \right\} \tag{3.31}$$

Where $\hat{W}_{ext}^e(\mathbf{v}^e)$ denotes the work done by the forces acting on the edges of e (either coming form f or $\mathbf{p_H}$). It is defined now the local minimisers $\hat{\mu}_h^e$ as,

$$\hat{\mu}_h^e = \min_{\mathbf{v}^e \in \underline{Z}_h^e} D_{\text{int}}^e(\mathbf{v}^e) = D_{\text{int}}^e(\hat{\hat{\mathbf{u}}}_h^e) \tag{3.32}$$

Proposition:

The minimiser $\hat{\mu}_h$ is

$$\hat{\mu}_h = \min_{e=1,\ldots m_H} \hat{\mu}_h^e \equiv \hat{\mu}_h^E \tag{3.33}$$

Proof

Consider any $\mathbf{v} \in \underline{\hat{X}}$ and let $\mathbf{v}^e$ denote its restriction to macroelement e. With this notation

$$D_{\text{int}}(\mathbf{v}) = \sum_e D_{\text{int}}^e(\mathbf{v}^e) \tag{3.34}$$

$$\hat{W}_{ext}(\mathbf{v}) = \sum_e \hat{W}_{ext}^e(\mathbf{v}^e) = 1 \tag{3.35}$$

then, we can follow the next reasoning

$$D_{\text{int}}(\mathbf{v}) = \sum_e D_{\text{int}}^e(\mathbf{v}^e) \tag{3.36}$$

$$= \sum_e \hat{W}_{ext}^e(\mathbf{v}^e) D_{\text{int}}^e\left(\frac{\mathbf{v}^e}{\hat{W}_{ext}^e(\mathbf{v}^e)}\right) \tag{3.37}$$

$$\geq \sum_e \hat{W}_{ext}^e(\mathbf{v}^e) D_{\text{int}}^e(\hat{\hat{\mathbf{u}}}_h^e) \tag{3.38}$$

$$\geq \hat{\mu}_h^E \sum_e \hat{W}_{ext}^e(\mathbf{v}^e) = \hat{\mu}_h^E \tag{3.39}$$

This implies that in the broken problem the deformation localizes in the weakest element. This is intuitively logical. Note that

$$\hat{\mathbf{u}}_h^e = 0 \ \ if \ e \neq E \ \text{ and } \ \hat{\mathbf{u}}_h^E = \hat{\hat{\mathbf{u}}}_h^E \tag{3.40}$$

3.5 Refinement procedure

The refinement process is based on the evaluation of the gap between lower and upper bound, this is

$$g = \mu_H - \hat{\mu}_h \tag{3.41}$$

In order to express this as the sum of positive element contributions note that

$$\mu_H = \sum_e D^e_{\text{int}}(\mathbf{u}^e_H) \tag{3.42}$$

$$\sum_e \hat{W}^e_{ext}(\mathbf{u}^e_H) = 1 \tag{3.43}$$

hence,

$$g = \sum_e (D^e_{\text{int}}(\mathbf{u}^e_H) - \hat{W}^e_{ext}(\mathbf{u}^e_H)\hat{\mu}_h) \tag{3.44}$$

The element gap is

$$g^e = D^e_{\text{int}}(\mathbf{u}^e_H) - \hat{W}^e_{ext}(\mathbf{u}^e_H)\hat{\mu}_h \tag{3.45}$$

To prove that it is always positive note that

$$D^e_{\text{int}}(\mathbf{u}^e_H) = \hat{W}^e_{ext}(\mathbf{u}^e_H) D^e_{\text{int}}\left(\frac{\mathbf{u}^e_h}{\hat{W}^e_{ext}(\mathbf{u}^e_h)}\right) \geq \hat{W}^e_{ext}(\mathbf{u}^e_H)\hat{\mu}^e_h \geq \hat{W}^e_{ext}(\mathbf{u}^e_H)\hat{\mu}^E_h \tag{3.46}$$

The element gap is an indicator of the contribution of each element to the total gap. The elements, which contribute more to the global gap, are the weakest ones. They will be refined. Note that the sum of all the element gaps is equal to the global gap

$$g = \sum_e g^e \tag{3.47}$$

The contribution of each element to the gab is defined by the percentage of the element gap to the global gap

$$\eta^e = \frac{g^e}{g} \tag{3.48}$$

Note that

$$\sum_e \eta^e = 1 \tag{3.49}$$

It has to be decided for which percentage we will refine the element. This is easy because the contribution of the elements which have not influence on the gap is very small. In the examples that appear in this paper it has been considered that a contribution of 10 % is a good ratio.

After the exposition of the method we have the capacity to apply it to the case of continuous beams under pure plastic bending and the case of continuous beams and frames under the combination of plastic bending and compression (or tension).

The refinement procedure is a fundamental step to understand the method. It implies that in order to converge to the approximation μ_c, in the refinement process the reference mesh has to be kept unchanged. That means that in the evaluation of the lower bound the number of elements that each element is subdivided depends on the mesh that has been used to calculate the upper bound in each refinement process. Besides, this number has to be such that, if all the elements are considered together once subdivided, the reference mesh used in equation (3.21) is obtained. This consideration ensures that we converge properly to μ_c. If the considered mesh is not accurate enough the value of μ_c may differ from the real collapse load.

Chapter 4. Continuous beam under pure plastic bending.

4.1 Introduction

The aim of this chapter is to express the equations of the method before exposed for the case of beams under pure plastic bending. This is the case of beams under loads normal to its longitudinal axis. The effect of shear or torsion is not considered. It is assumed that there is plastic deformation everywhere, although this turns out to be very small except at hinges.

4.2 Discretisation

A two nodes bar element with two degrees of freedom (v_i, θ_i) in each node is used in the discretisation of the structure. O.C. Zienkiewicz (1967) has been one of the most important contributor to the finite element method. In this work we use a simple bar element, but all the concepts related to the finite element method appear.

A cubic polynomial is used to interpolate the vertical displacement. The local x axis is considered longitudinal to the bar. The other two axis are the principal axis of the section. Note that the loads have to act in the direction of the principal axis.

$$v(x) = a_3 x^3 + a_2 x^2 + a_1 x + a_0 \tag{4.1}$$

The next step is to express (4.1) in function of the nodal degrees of freedom. Figure (4.1) show the sign criteria of the displacements and the internal forces.

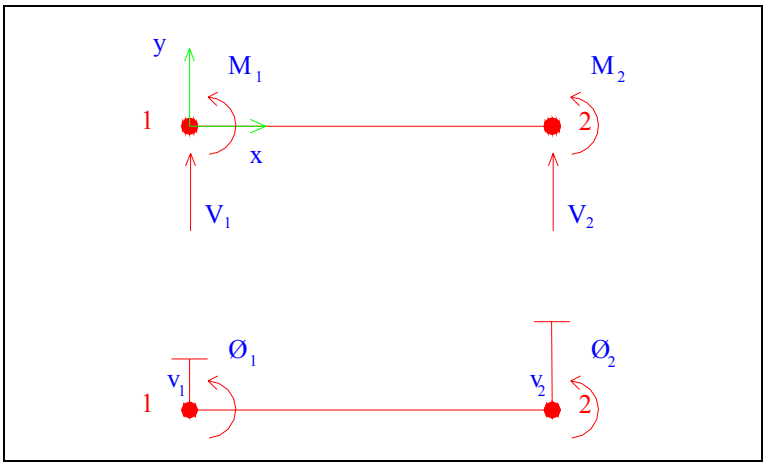

Figure 4.1 Local axis, internal forces and displacements. Sign criteria.

After solving a linear system, it is obtained the following standard expression,

$$v(x) = N_1(x)v_1 + N_2(x)\theta_1 + N_3(x)v_2 + N_4(x)\theta_2 \tag{4.2}$$

where the functions $N_i(x)$ are called the *shape functions*. In this case the shape functions are the Hermite polynomials.

$$N_1 = 1 - 3\left(\frac{x}{l^e}\right)^2 + 2\left(\frac{x}{l^e}\right)^3 \tag{4.3}$$

$$N_2 = x\left(1 - \frac{x}{l^e}\right)^2 \tag{4.4}$$

$$N_3 = 3\left(\frac{x}{l^e}\right)^2 - 2\left(\frac{x}{l^e}\right)^3 \tag{4.5}$$

$$N_2 = \left(x - l^e\right)\left(1 - \frac{x}{l^e}\right)^2 \tag{4.6}$$

The displacement **v** can be expressed in matrix notation as,

$$v(x) = [N_1(x) \quad N_2(x) \quad N_3(x) \quad N_4(x)]\begin{bmatrix} v_1 \\ \theta_1 \\ v_2 \\ \theta_2 \end{bmatrix} = \mathbf{N}^T(x)\mathbf{v} \tag{4.7}$$

We will obtain expressions for the power equilibrium equation given by

$$W_{ext} = D_{\text{int}} \tag{4.8}$$

which express the equilibrium between the plastic dissipation in the structure and the work done by the external loads.

4.3 Plastic element dissipation

Let's find the right hand side of equation (4.8). It has been mentioned before that the plastic dissipation is

$$D_{\text{int}} = \int_{V^e} \sigma \dot{\varepsilon}_p \, dV \tag{4.9}$$

where the integral is along all the structure.

Now, if expression (4.9) is referred to the structural mesh,

$$D_{\text{int}} = \sum_e \int_{V^e} \sigma \dot{\varepsilon}_p \, dV \tag{4.10}$$

where

$$D^e_{\text{int}} = \int_{l^e}\int_{A^e} \sigma(z)\dot{\theta}\, z dA dx = \int_{l^e}\int_{A^e} \sigma(z) z dA \dot{\theta}\, dx = \int_{l^e} M^e \dot{\theta}\, dx \tag{4.11}$$

finally, using that the curvature can be obtained from the vertical displacement expression (4.11) turns into,

$$D_{\text{int}}^{e} = \int_{l^e} M^e \dot{\theta}\, dx = M_p^e \int_{l^e} |\dot{\theta}|dx = M_p^e \int_{l^e} \left|\frac{d^2 v^e}{dx^2}\right| dx \tag{4.12}$$

In our mesh it is considered that the elements are fully plasticized. In this case it can be worked out the plastic dissipation in one element as a function of the absolute value of the torsion and the plastic moment of the element

$$D_{\text{int}}^{e} = \int_{l^e} M_p^e \left|\frac{d^2 v^e}{dx^2}\right| dx \tag{4.13}$$

Note that it is supposed that the element has constant plastic moment in order to simplify the integral. If equation (4.7) is introduced into equation (4.13), the plastic dissipation is expressed in matrix notation.

$$\frac{d^2 v^e}{dx^2}(x) = \frac{d^2 \mathbf{N}^T}{dx^2}(x)\mathbf{v}^e = \mathbf{B}^T(x)\mathbf{v}^e \tag{4.14}$$

where

$$\mathbf{B}(x) = \begin{bmatrix} \frac{d^2 N_1}{dx^2}(x) \\ \frac{d^2 N_2}{dx^2}(x) \\ \frac{d^2 N_3}{dx^2}(x) \\ \frac{d^2 N_4}{dx^2}(x) \end{bmatrix} \text{ and } \mathbf{v}^e = \begin{bmatrix} v_1 \\ \theta_1 \\ v_2 \\ \theta_2 \end{bmatrix}^e \tag{4.15}$$

and the plastic dissipation in one element is

$$D_{\text{int}}^{e} = \int_{l^e} M_p^e \left|\mathbf{B}^T(x)\mathbf{v}^e\right| dx = M_p^e \int_{l^e} \left|\mathbf{B}^T(x)\mathbf{v}^e\right| dx \tag{4.16}$$

It is important to note that to work with the absolute value of a function it is difficult. Therefore, it will be replaced by an equivalent numerical expression. This is by simply square the function and then take the square root of it. Then (4.16) turns into

$$D_{\text{int}}^{e} = M_p^e \int_{l^e} \sqrt{(\mathbf{B}^T(x)\mathbf{v}^e)^2}\, dx \tag{4.17}$$

Then, the total internal dissipation in the structure is

$$D_{\text{int}} = \sum_e M_p^e \int_{l^e} \sqrt{(\mathbf{B}^T(x)\mathbf{v}^e)^2}\, dx \tag{4.18}$$

Let's now find the left hand side of equation (4.8).

4.4 External loads work.

The work of the external loads is well described by equation (2.15), which it is recalled now for the case of a bar structure. It is considered only distributed loads and point loads. Expression (4.19) takes into account the contribution of the moments that can load the structure in different points.

$$W_{ext}^{e} = \int_{l^e} t^e(x)\, v\ (x)\, dS + \sum_{i}^{n} F_i^e\, v(x_i) + \sum_{i}^{k} M_i^e\, \theta(x_i) \tag{4.19}$$

where *t(x)* represent the distributed loads, F_i represent the point loads acting in the x_i points and M_i represent the point moment acting in x_i i.. To obtain a simplified integral it is supposed that within one element the distributed loads do not change with *x*.

Considering proportional loading and that μ_k is the proportional multiplier, expression (4.19) can be expressed in matrix notation as,

$$\begin{aligned} W_{ext}^{e} &= \mu_k [(\hat{\mathbf{F}}_1^{t\,T} + \hat{\mathbf{F}}_1^{F\,T} + \hat{\mathbf{F}}_1^{M\,T})^e \quad (\hat{\mathbf{F}}_2^{t\,T} + \hat{\mathbf{F}}_2^{F\,T} + \hat{\mathbf{F}}_2^{M\,T})^e] \begin{bmatrix} \mathbf{v}_1^e \\ \mathbf{v}_2^e \end{bmatrix} \\ &= [\hat{\mathbf{F}}_1^{e\,T} \quad \hat{\mathbf{F}}_2^{e\,T}] \begin{bmatrix} \mathbf{v}_1^e \\ \mathbf{v}_2^e \end{bmatrix} = \mu_k \hat{\mathbf{f}}^{e\,T} \mathbf{v}^e = \mu_k \hat{W}_{ext}^{e} \end{aligned} \tag{4.20}$$

Where $\hat{\mathbf{F}}_i^{j}$ are the external nodal loads and $\mathbf{v}_i$ are the nodal degrees of freedom.
Then, the total external work is

$$W_{ext} = \mu_k \sum_{e} \hat{W}_{ext}^{e} = \mu_k \hat{W}_{ext} \tag{4.21}$$

Our variables are the multiplier μ_k and the nodal degrees of freedom (v_i, θ_i).

4.5 Optimization problem.

Combining the power equality with the definitions given by equations (4.12) and (4.21), the load multiplier can be expressed as,

$$\mu_k = \frac{D_{\text{int}}}{\hat{W}_{ext}} \tag{4.22}$$

as we want the minimum multiplier

$$\mu_k = \min_{\mathbf{v} \in X_H} \frac{D_{\text{int}}}{\hat{W}_{ext}}(\mathbf{v}) \tag{4.23}$$

Expression (4.23) can be simplified if the reduced space of displacements given by (3.20) is considered. Now, our problem is

$$\mu_k = \min_{\mathbf{v}\in \underline{X}_H} D_{\text{int}}(\mathbf{v}) \tag{4.24}$$

subjected to

$$\hat{W}_{ext}(\mathbf{v}) = 1 \tag{4.25}$$

In the following lines, the stiffness matrix for one element will be found. In order to assemble the stiffness matrix of the structure, a standard stiffness method will be used. This method uses nodal equilibrium and displacements compatibility.

Using the Lagrange multiplier method to find the minimum of equation (4.24) with restriction (4.25), the following expression is found

$$\hat{D}_{\text{int}}(\mu_k, \mathbf{v}\ ) = D_{\text{int}}(\mathbf{v}) - \mu_k(\hat{\mathbf{f}}^{\ T}\mathbf{v}\ - 1) = 0 \tag{4.26}$$

Now, taking the derivation of equation (4.26), the following to equations are obtained.

First, if we make the derivation respect the multiplier

$$\frac{\partial \hat{D}_{\text{int}}}{\partial \mu_k}(\mu_k, \mathbf{v}\ ) = \hat{\mathbf{f}}^{\ T}\mathbf{v}\ - 1 = 0 \tag{4.27}$$

equation (4.25) is obtained.

Second, the following expression is obtained by taking the derivation of (4.26) respect the nodal displacements

$$\frac{\partial \hat{D}_{\text{int}}}{\partial \underline{v}}(\mu_k, \mathbf{v}\ ) = \frac{\partial D_{\text{int}}}{\partial \mathbf{v}}(\mathbf{v}\ ) - \mu_k \hat{\mathbf{f}}\ = 0 \tag{4.28}$$

Finally, expression (4.29) gives us the non-linear system that must be solved to obtain the load multiplier and the nodal degrees of freedom.

$$\frac{\partial D_{\text{int}}}{\partial \mathbf{v}}(\mathbf{v}\ ) = \mu_k \hat{\mathbf{f}} \tag{4.29}$$

Now, the stiffness matrix of one element is given by (4.30)

$$\frac{\partial D^e_{\text{int}}}{\partial \mathbf{v}^e}(\mathbf{v}^e) = M^e_p \frac{\partial}{\partial \mathbf{v}^e}\left(\int_{l^e} \sqrt{(\mathbf{B}^T(x)\mathbf{v}^e)^2}\, dx\right) \tag{4.30}$$

as the limits of integration do not depend on $\mathbf{v}^e$, expression (4.30) can be change for

$$\frac{\partial D^e_{\text{int}}}{\partial \mathbf{v}^e}(\mathbf{v}^e) = M^e_p \int_{l^e} \frac{\partial}{\partial \mathbf{v}^e}\left(\sqrt{(\mathbf{B}^T(x)\mathbf{v}^e)^2}\right)dx =$$

$$= M^e_p \int_{l^e} \frac{1}{\sqrt{(\mathbf{B}^T(x)\mathbf{v}^e)^2}} \mathbf{B}(x)\mathbf{B}^T(x)\mathbf{v}^e dx$$

$$= M^e_p \left(\int_{l^e} \frac{1}{\sqrt{(\mathbf{B}^T(x)\mathbf{v}^e)^2}} \mathbf{B}(x)\mathbf{B}^T(x)dx\right)\mathbf{v}^e = \mathbf{k}^e(\mathbf{v}^e)\mathbf{v}^e \qquad (4.31)$$

where $\mathbf{k}^e(\mathbf{v}^e)$ is the local stiffness matrix of the element.

$$\mathbf{k}^e(\mathbf{v}^e) = M^e_p \int_{l^e} \frac{1}{\sqrt{(\mathbf{B}^T(x)\mathbf{v}^e)^2}} \mathbf{B}(x)\mathbf{B}^T(x)dx \qquad (4.32)$$

$$\mathbf{k}^e(\mathbf{v}^e) = M^e_p \int_{l^e} \begin{bmatrix} \frac{d^2N_1}{dx^2}\frac{d^2N_1}{dx^2} & \frac{d^2N_1}{dx^2}\frac{d^2N_2}{dx^2} & \frac{d^2N_1}{dx^2}\frac{d^2N_3}{dx^2} & \frac{d^2N_1}{dx^2}\frac{d^2N_4}{dx^2} \\ \frac{d^2N_2}{dx^2}\frac{d^2N_1}{dx^2} & \frac{d^2N_2}{dx^2}\frac{d^2N_2}{dx^2} & \frac{d^2N_2}{dx^2}\frac{d^2N_3}{dx^2} & \frac{d^2N_2}{dx^2}\frac{d^2N_4}{dx^2} \\ \frac{d^2N_3}{dx^2}\frac{d^2N_1}{dx^2} & \frac{d^2N_3}{dx^2}\frac{d^2N_2}{dx^2} & \frac{d^2N_3}{dx^2}\frac{d^2N_3}{dx^2} & \frac{d^2N_3}{dx^2}\frac{d^2N_4}{dx^2} \\ \frac{d^2N_4}{dx^2}\frac{d^2N_1}{dx^2} & \frac{d^2N_4}{dx^2}\frac{d^2N_2}{dx^2} & \frac{d^2N_4}{dx^2}\frac{d^2N_3}{dx^2} & \frac{d^2N_4}{dx^2}\frac{d^2N_4}{dx^2} \end{bmatrix}(x)dx \qquad (4.33)$$

In this work, a Gauss-Legendre quadrature has been used to integrate the element stiffness matrix along the element.

$$\mathbf{k}^e(\mathbf{v}^e) = \sum_i^{ngauss} C_i \frac{M^e_p l^e}{2\sqrt{\varepsilon^2 + (\mathbf{B}^T(\xi_i)\mathbf{v}^e)^2}} \mathbf{B}(\xi_i)\mathbf{B}^T(\xi_i) \qquad (4.34)$$

Note that a change of variable has been used. It has been changed $x \in [0, l^e]$ to the variable $\xi \in [-1, 1]$. The jacobian of the change is $\frac{l^e}{2}$. In the examples presented in this thesis a two nodes quadrature has been used.

Notice that the parameter ε has been introduced in order not to divide by zero. This happens for that elements where the plastic deformation is very small or zero. The value of ε has to be small enough compared to the other term in the square root sign. In the examples that we present its value is 10^{-5}.

Once assembled the stiffness matrix of the structure, equation (4.29) and (4.27) can be expressed as,

$$\mathbf{K}(\mathbf{v})\mathbf{v} = \mu_k \hat{\mathbf{f}} \qquad (4.35)$$

$$\hat{\mathbf{f}}^T \mathbf{v} = 1 \tag{4.36}$$

These equations describe a non-linear system in local global axis. That means, in this case, that the system matrix depends on the variable we want to find. In this work it has been used the Picard's method to solve the non-linear set of equations. It will be described in a future section.

The methodology to solve equations (4.35) and (4.36) is explained by the following equations. First let's divide (4.35) by μ_k.

$$\mathbf{K}(\mathbf{v})\frac{\mathbf{v}}{\mu_k} = \hat{\mathbf{f}} \rightarrow \mathbf{K}(\mathbf{v})\mathbf{v}_o = \hat{\mathbf{f}} \tag{4.37}$$

Now using Picard's method we will find $\mathbf{v}_o$. Then, the displacements are

$$\mathbf{v}^e = \mu_k \mathbf{v}_o \tag{4.38}$$

Substituting equation (4.38) into equation (4.36)

$$\hat{\mathbf{f}}^T \mathbf{v} = \mu_k \hat{\mathbf{f}}^T \mathbf{v}_o = 1 \tag{4.39}$$

which enables, the value of the multiplier that gives us an upper bound of the collapse load, to be evaluated as,

$$\mu_k = \frac{1}{\hat{\mathbf{f}}^T \mathbf{v}_o} \tag{4.40}$$

4.6 Solving the nonelinear system. Picard's method. Upper bound evaluation.

Let's consider a general non-linear system **A(x)x=b(x)**. Figure 4.2 show how the Picard's method works.

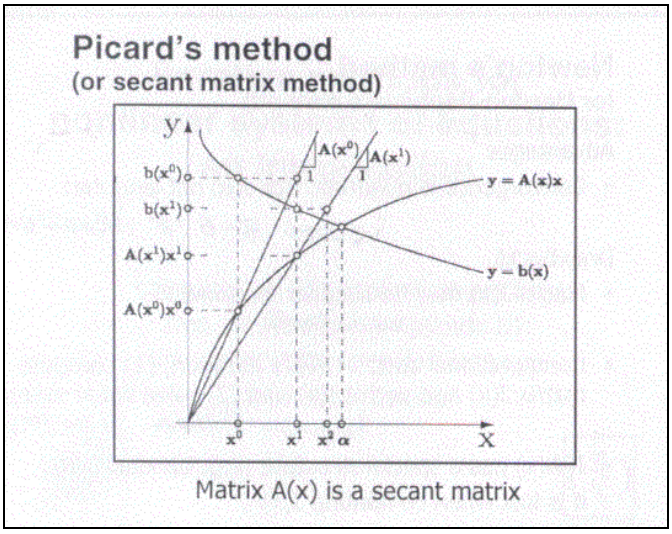

Figure 4.2 Picard's method

Picard's method consist on selecting an initial guess $\mathbf{v}^o$ for the displacement vector $\mathbf{v}$. Then an initial secant matrix $\mathbf{k}(\mathbf{v}^o)$ can be obtained. Now, the procedure expressed by equations (4.37)-(4.40) to find $(\mathbf{v}^1, \mu_k^1)$ can be applied. The process is as follows,

Initial guess $\mathbf{v}^o$

$$\mathbf{v}^o \rightarrow \mathbf{K}(\mathbf{v}^o)$$

then until convergence

$$\mathbf{K}(\mathbf{v}^k)\frac{\mathbf{v}^{k+1}}{\mu_k^{k+1}} = \hat{\mathbf{f}} \rightarrow \mathbf{K}(\mathbf{v}^k)\mathbf{v}_0^{k+1} = \hat{\mathbf{f}} \tag{4.41}$$

$$\mu_k^{k+1} = \frac{1}{\hat{\mathbf{f}}^T \mathbf{v}_o^{k+1}} \tag{4.42}$$

$$\mathbf{v}^{k+1} = \mu_k^{k+1}\mathbf{v}_o^{k+1} \tag{4.43}$$

In Picard's method we have transformed a non-linear problem into a linear one. Now, the problem turns into how to solve a linear system. As for non-linear systems, there are several methods of solving it. In our case the stiffness matrix of the structure is symmetric and positive defined. So, it seems logical to use a method that takes advantage of these properties. But, in the iterative process explained before the symmetry of the matrix can be guaranteed, but it may not be positive defined for some values of the approximation of the displacement vector introduced in it. This fact is one of the causes of the reduction in the velocity of convergence of the method used. It has been implemented a triangular (LU) factorization of the matrix in order to solve the linear system. Therefore we use a direct method to solve the linear system.

In the developed program the stiffness matrix is first stored in a profile form. Then the subroutine **datri** is used to make the triangular factorization. Finally, the subroutine **dasol** is used to carry out the back-substitution.

Let's now focus on the convergence control. Control of convergence must be done for two elements: $\mathbf{v}$ and μ_k. Two tolerances are defined: t_v (tolerance for $\mathbf{v}$) and t_u (tolerance for μ_k). These tolerances will depend on the number of significant figures q we need. We define the tolerance for q significant figures as

$$t = \frac{1}{2}10^{-q} \tag{4.44}$$

Now the relative errors can be defined, these will be compared to the tolerances.

$$e_v = \frac{\| \mathbf{v}^{k+1} - \mathbf{v}^k \|}{\| \mathbf{v}^{k+1} \|} \tag{4.45}$$

$$e_{\mu} = \frac{\| \mu_k^{k+1} - \mu_k^k \|}{\| \mu_k^{k+1} \|} \qquad (4.46)$$

4.7 Lower bound evaluation. Element equilibrium

Once convergence has been reached for both variables **v** and μ_k, the following step is the evaluation of the lower bound of the collapse load.

First, we will isolate each element with its external loads and nodal internal loads. Second, isostatic boundary conditions will be introduced to the element nodes. This is necessary for being able to apply the procedure before explained to work out the upper bound of the element. These conditions are introduced in order to avoid having a singular stiffness matrix. As the external loads are in equilibrium with the nodal internal loads, the reactions of this local problem are zero. Finally, once all the upper bounds of all the elements have been worked out, the minimum of all theses multipliers is the lower bound of the collapse load approximation μ_c.

A mesh has to be proposed for each element. The number of elements that will be used in the mesh of one element cannot be arbitrary as it has been explained in chapter 3. This number has to satisfy the condition that the reference mesh of the structure towards we want to converge does not change.

Let's say that *nelem2* is the number of elements that will be used to subdivide one element of the structure model in one particular refinement step. This number will change from element to element in order to keep constant the reference mesh mentioned before. Figure (4.3) tries to explain this idea. Let's say that it begins with *nelem2* for each element. This means that *nelem2* is the number of elements that will be used to calculate the lower bound in each element. If it is considered that the elements that have to be subdivided are divided in two new elements, then, let's say that element 2-3 is the only one that has to be subdivided. The other elements will keep nelem2 for the lower bound in the next step, but element 2-3 turn into 2-6 and 6-3. These two elements will have $\frac{nelem2}{2}$. And if 6-3 has to be subdivided in the next step, elements 6-7 and 7-3 will have $\frac{nelem2}{4}$, while the other elements keep the values of the step before. When calculating the lower bound, the number of elements, that will be used in those elements that have been refined in the iteration before, has to be reduced. This is very important in order to be consistent when compare the lower and upper bound through the refinement process.

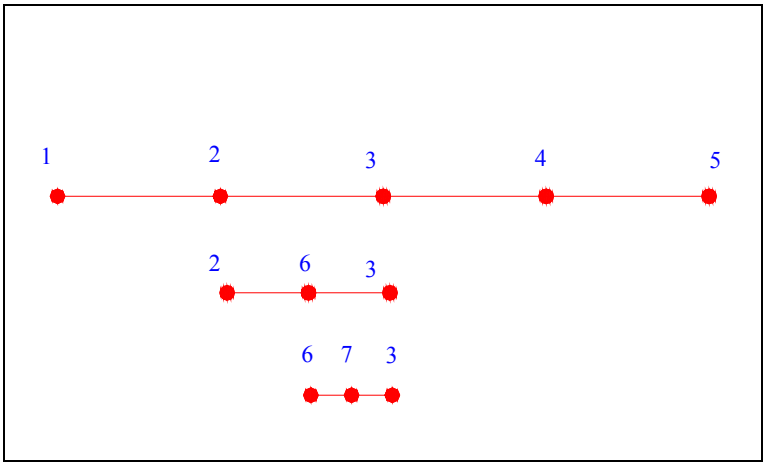

Figure 4.3 Refinement process

Then, next step is to work out the nodal internal loads in each element. These are given by equation (4.47) for the element *ij*.

$$\mu_k \begin{bmatrix} \hat{\mathbf{F}}_1^{ij} \\ \hat{\mathbf{F}}_2^{ij} \end{bmatrix} = \begin{bmatrix} \mathbf{k}_{11}^{ij} & \mathbf{k}_{12}^{ij} \\ \mathbf{k}_{21}^{ij} & \mathbf{k}_{22}^{ij} \end{bmatrix} \begin{bmatrix} \mathbf{v}_1^{ij} \\ \mathbf{v}_2^{ij} \end{bmatrix} - \mu_k \begin{bmatrix} \hat{\mathbf{F}}^{t\,ij}_1 + \hat{\mathbf{F}}^{F\,ij}_1 + \hat{\mathbf{F}}^{M\,ij}_1 \\ \hat{\mathbf{F}}^{t\,ij}_2 + \hat{\mathbf{F}}^{F\,ij}_2 + \hat{\mathbf{F}}^{M\,ij}_2 \end{bmatrix} \tag{4.47}$$

In summary, the internal loads are given by the difference between the internal loads due to the power dissipation and the nodal element loads due to the external loads.

Let's now proof that one given element has to be in equilibrium.

The equilibrium equation between the external and internal power tells us that the internal loads have to be in equilibrium with the external loads acting in the element. But, what is not so trivial is the reason that the loads given by equation (4.48) must be in equilibrium. Given the element *ij*

$$\begin{bmatrix} \hat{\mathbf{T}}_1^{ij} \\ \hat{\mathbf{T}}_2^{ij} \end{bmatrix} = \begin{bmatrix} \mathbf{k}_{11}^{ij} & \mathbf{k}_{12}^{ij} \\ \mathbf{k}_{21}^{ij} & \mathbf{k}_{22}^{ij} \end{bmatrix} \begin{bmatrix} \mathbf{v}_1^{ij} \\ \mathbf{v}_2^{ij} \end{bmatrix} \tag{4.48}$$

in a more compact notation,

$$\mathbf{T} = \mathbf{k}(\mathbf{v})\mathbf{v} \tag{4.49}$$

Where **v** is the displacement vector after convergence.

On the one hand, if the stiffness matrix multiplies an arbitrary rigid body displacement, then, this product is zero.

$$\mathbf{k}(\mathbf{v})\mathbf{u}_R = 0 \tag{4.50}$$

On the other hand, the following expression proves that the nodal loads **T** must be in equilibrium. Let's multiply (4.49) by an arbitrary rigid body displacement.

$$\mathbf{u}_R^T\mathbf{T} = \mathbf{u}_R^T(\mathbf{k}(\mathbf{v})\mathbf{v}) = \mathbf{v}(\mathbf{k}(\mathbf{v})\mathbf{u}_R) = 0 \tag{4.51}$$

then,

$$\mathbf{u}_R^T \mathbf{T} = \mathbf{T}^T \mathbf{u}_R = 0 \tag{4.52}$$

Equation (4.52) implies equilibrium.

4.8 Refinement process

Once the upper and lower bound of the collapse load for the proposed mesh have been found, the next step is to propose a a new mesh that will give a more accurate upper and lower bound values.

Equation (3.45) give us the expression of the element gap. The percentage of contribution of each element can be found. The element contribution percentage will be compared to a percentage of reference. All the elements that have bigger contribution than the reference contribution will be refined.

One of the aim of this work is to have a mesh with lot of elements where the hinges form and few elements were they do not. In the examples presented in this work the elements have been divided into two new elements. We do not want to create a huge number of elements that will not contribute to improve the upper and lower bound.

When the new mesh is set, the process starts from the beginning until the lower and upper bounds are close enough.

Let's point out that because we subdivide one element into two new elements, then the number of elements in the very refined mesh considered in chapter 4 should be a power of 2. Let's say 2^n, where n is a positive integer. This is important in order to keep as an integer the number of elements used when working out the lower bound.

4.9 Examples

The following examples show how the upper bound and lower bound converge towards each other. In some of the examples we compare both values to the real collapse load, and therefore, they are presentedan unitary diagram. In more complicated examples we do not have the real collapse load, so the lower bound and upper bound values are compared.

In all the examples, convergence has been achieved with seven significant figures. And the parameter ε, that has been introduced to avoid dividing by zero, is 10^{-5}.

It is interesting to see how the elements concentrate where the plastic deformations concentrates. Then, the cross sections where the plastic hinges form are the ones where the elements concentrate.

Example1

Section properties:

Rectangular cross section:

h =0.1 m

b= 0.05 m

Limit elastic: $\sigma_y = 275000000 \ \ Pa$

Let's consider first the easy example shown in figure 4.4

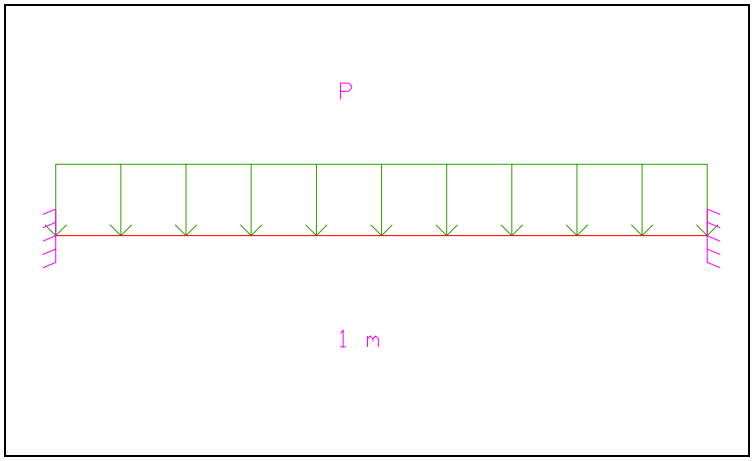

Figure 4.4 Beam with distributed load

Figure 4.5 shows us the real mechanism of collapse of the beam. When running the programme it is found that the elements concentrate where the hinges are supposed to appear.

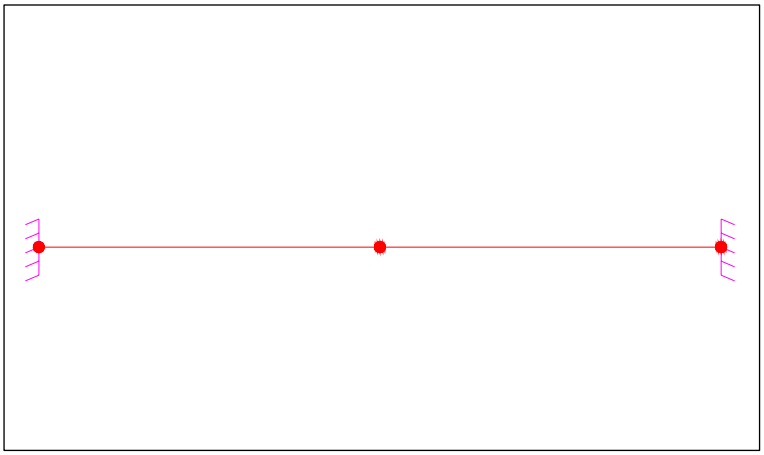

Figure 4.5 Mechanism of collapse

Figure 4.6 show that the elements concentrate where the hinges form.

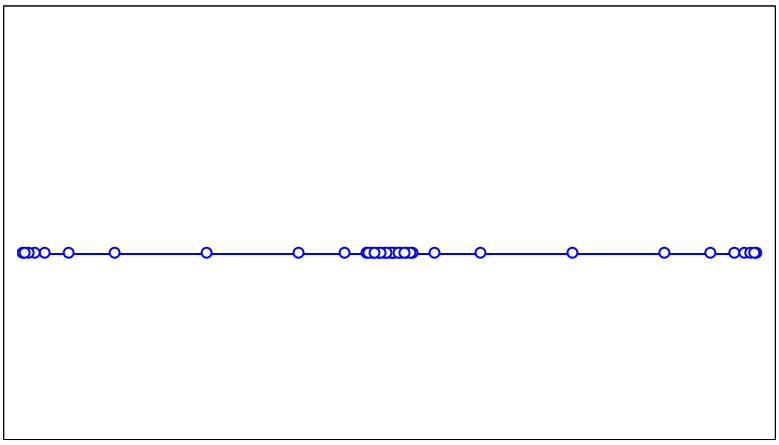

Figure 4.6 Mesh 28 elements

Figure 4.7 shows the unitary convergence of the lower and upper bounds towards the collapse load when a reference mesh of 256 equally distributed is considered. These values have been compared with the real collapse load $\frac{16Mp}{L^2} = 550000\ N$. This Figure tells us that the consideration of 256 elements is accurate enough.

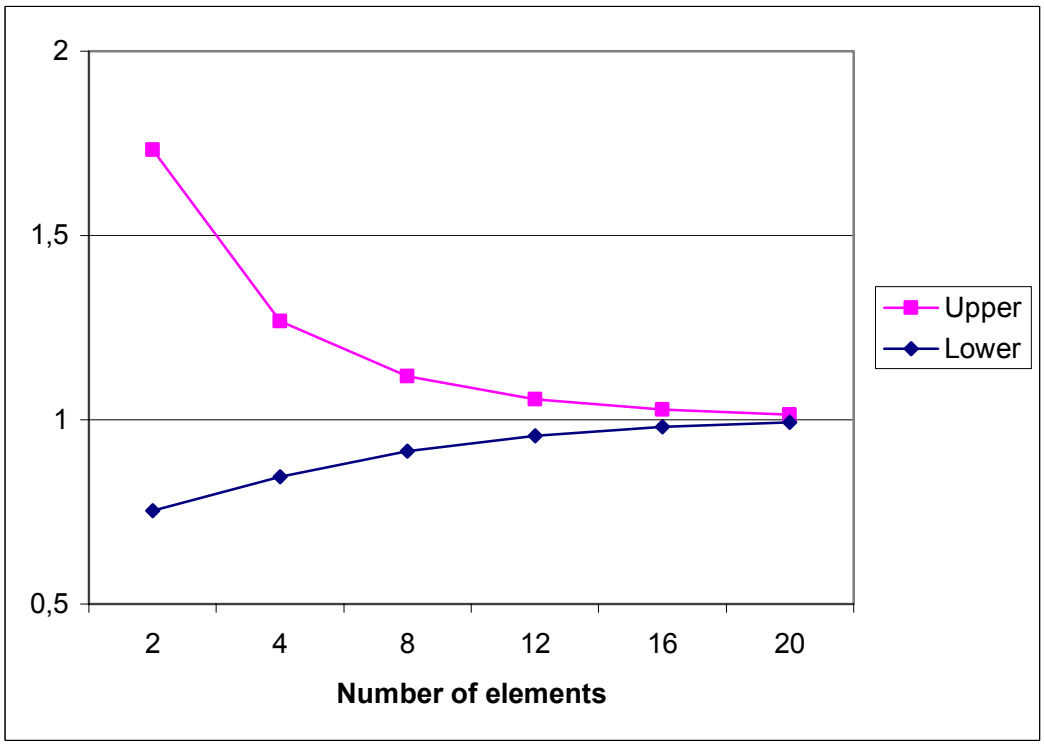

Figure 4.7 Convergence Upper bound-Lower bound

Table 4.1 shows the values of the upper and lower bounds we have obtained. You can notice that they converge towards the real collapse load.

Number of elements	Upper bound (N)	$\frac{Upper\ bound}{Collapse\ Load}$	Lower bound (N)	$\frac{Lower\ bound}{Collapse\ Load}$
2	952627,9	1,73205	414566,3	0,75375
4	697372,3	1,26795	465171,6	0,84576
8	614983,7	1,11815	502997,6	0,91454
12	580692,6	1,05580	526424,8	0,95713
16	564984,6	1,02724	539568,4	0,98103
20	557535,7	1,01370	546618,5	0,99385

Table 4.1 Upper bound and Lower bound values

If a mesh with less than 256 elements as the reference mesh is considered. It is possible to have lower bounds bigger than the real collapse load, but it is not possible to have upper bounds lower than the real collapse load. This reflects what it has been said along this work. The method is based on a supposed initial reference mesh. The accuracy of the results depends on this mesh. In Table 4.2 this fact can be seen. This values have been obtained supposing a fine mesh of 128 elements. Note that a lower bound value bigger than the real collapse load is obtained.

Number of elements	Upper bound (N)	$\frac{Upper\ bound}{Collapse\ Load}$	Lower bound (N)	$\frac{Lower\ bound}{Collapse\ Load}$
2	952627,9	1,73205	416627,5	0,75750
4	697372,3	1,26795	467770,3	0,85049
8	614983,7	1,11815	506038,8	0,92007
12	580692,6	1,05580	529757,5	0,96319
16	564984,6	1,02724	543070,4	0,98740
20	557535,7	1,01370	550213,1	**1,00038**

Table 4.2 Upper bound and lower bound values

Example 2

Section properties:

Rectangular cross section:
h =0.1 m
b= 0.05 m
Limit elastic: $\sigma_y = 275000000\ \ Pa$

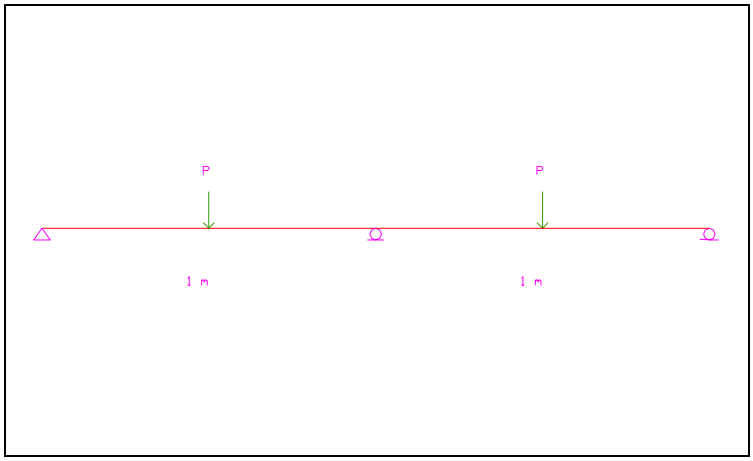

Figure 4.8 2-Span Beam

The mechanism of collapse is shown in figure 4.9. The plastic hinges appear where the point loads act and in the middle support.

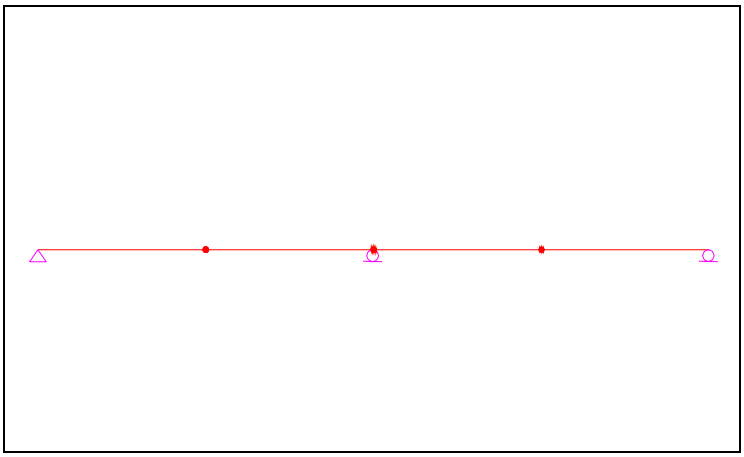

Figure 4.9 Mechanism of collapse

And figure 4.10 shows how the elements concentrate where the hinges are supposed to appear.

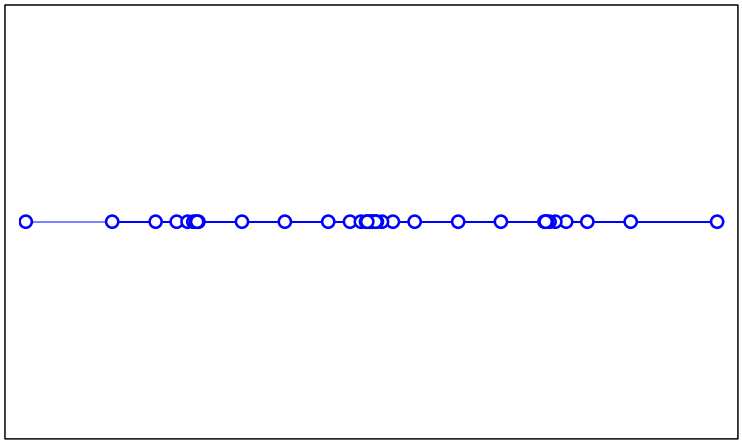

Figure 4.10 Mesh 28 elements

Finally, Figure 4.11 and table 4.3 show the convergence of the upper bound and the lower bound.

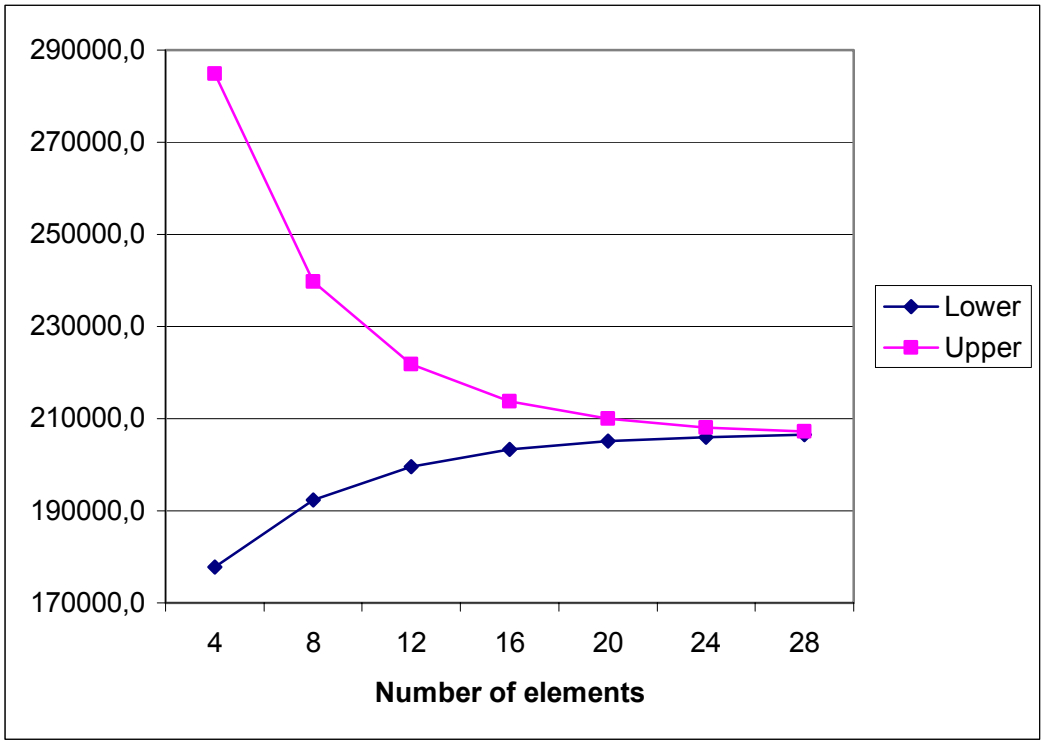

Figure 4.11 Convergence Upper bound-Lower bound

Number of elements	*Upper bound (N)*	*Lower bound (N)*
4	284872,2	177728,300000
8	239700,4	192334,24000
12	221803,2	199638,7000
16	213763,3	203292,40000
20	209945,7	205120,20000
24	208086,4	206035,80000
28	207169,9	206489,50000

Table 4.3 Upper bound and Lower bound values

Example 3

Section properties:

Rectangular cross section:
h =0.1 m
b= 0.05 m
Limit elastic: $\sigma_y = 275000000 \ \ Pa$

Let's consider now a more general example as the one in Figure 4.12.

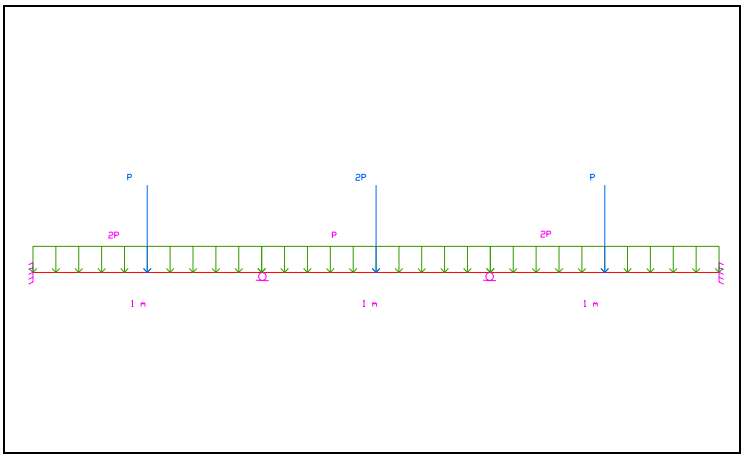

Figure 4.12 3-Span Beam

The real mechanism of collapse is shown in figure 4.13.

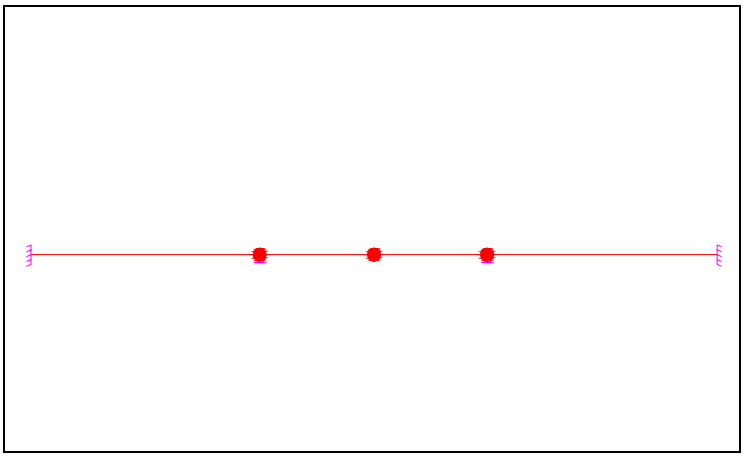

Figure 4.13 Mechanism of collapse

As we expect, figure 4.14 shows us how the elements concentrate where the real mechanism has its plastic hinges.

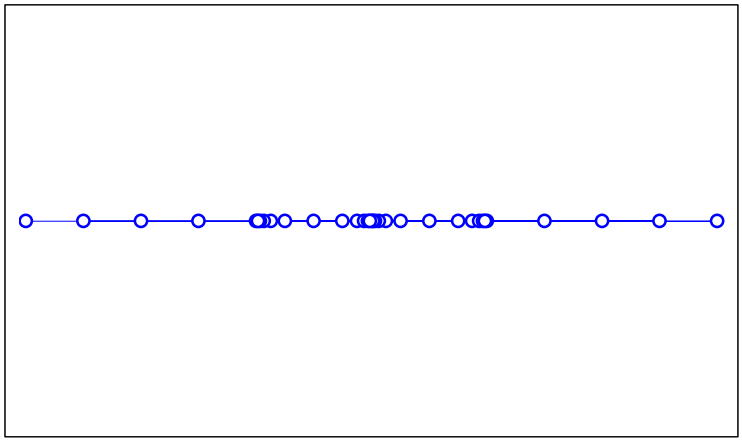

Figure 4.14 Mesh 24 elements

Finally figure 4.15 and table 4.4 show us the expected behavior of the upper and lower bounds.

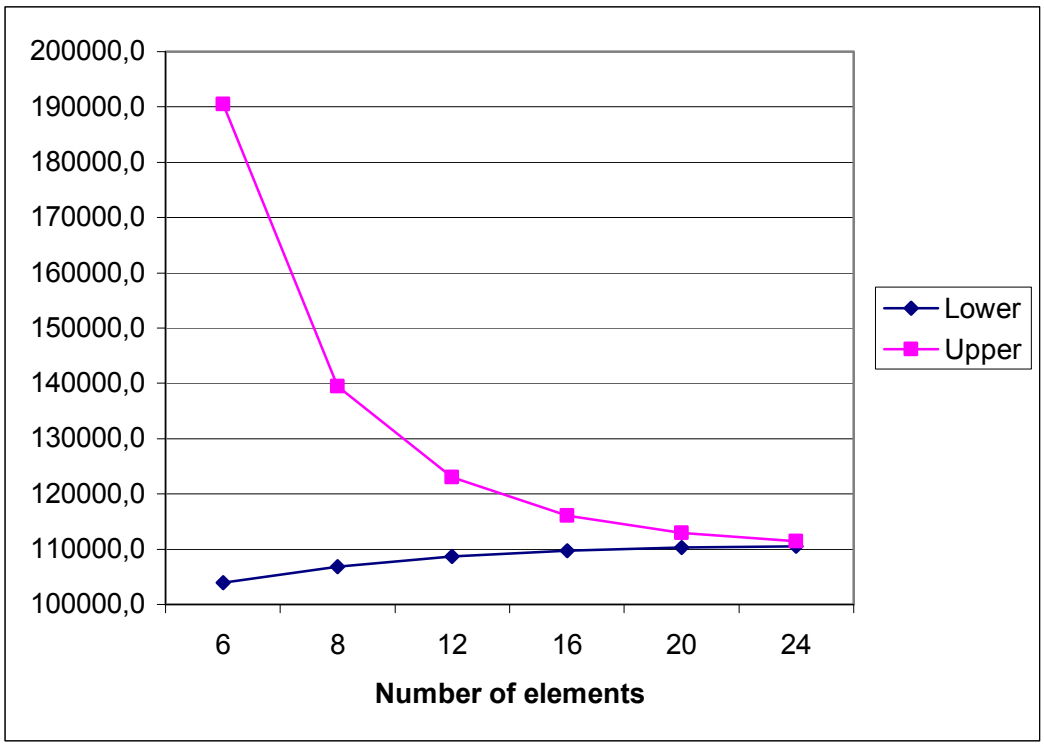

Figure 4.15 Convergence Upper bound-Lower bound

Number of elements	*Upper bound (N)*	*Lower bound (N)*
6	190525,8	103896,7
8	139474,4	106808,9
12	122996,1	108685,6
16	116135,6	109740,5
20	112984,6	110298,8
24	111472,5	110586,0

Table 4.4 Upper bound and Lower bound values

Chapter 5. Plastic analysis of structures under uniaxial stress. Combined plastic bending and compression or tension.

The next hypothesis is considered in chapter 5 and 6:

- We apply the deformation theory of plasticity, which states that the strain has the same sign as the stress. The stress state is entirely determined by the current strain state, independently of the previous history of strain evolution (Hencky, 1924). This supposition is accurate enough in our case because the loading process is monotonic.

5.1 Generalized plastic hinge.

Since now it has been assumed that the plastic hinge forms when the bending moment reaches the plastic limit value, M_o. It has been neglected other effects as the contribution of the axial internal force or the share internal force. In this section it is considered only the effect of the normal force N. This effect it is important in multi-storey frames or frames with a large horizontal thrust where the axial forces are large.

Figure (5.1) shows the typical evolution of the strain and stress profiles during the formation of the generalized plastic Hinge. Note that the strain distribution is linear. The stress is linear only in the elastic zone (Figure 5.1.(a)). In the plastic zone the stress has a constant value σ_o, positive or negative. As the loading process continues, yielding starts at the top or bottom fibers, and the plastic zone propagates into the interior of the cross section (Figure (5.1(b)). For very large curvatures, the elastic zone becomes negligible small, and the stress distribution approaches a piecewise constant distributions, with one part of the cross section yielding in tension and the remaining part yielding in compression.

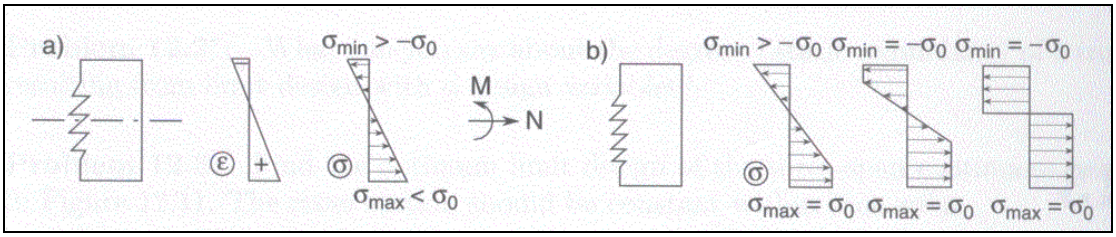

Figure 5.1 Strain and stress distributions

In order to work out the plastic dissipation we have to formulate an expression for the plastic strain. Due to that only bending and normal force are considered, the displacement in the direction of the bar *u* can be expressed as follows

$$u(x,y,z) = u(x) - y\frac{\partial v(x)}{\partial x} = u(x) - y\theta(x) \qquad (5.1)$$

where *u(x)* is the longitudinal displacement due to normal forces and *v(x)* is the bending displacement.

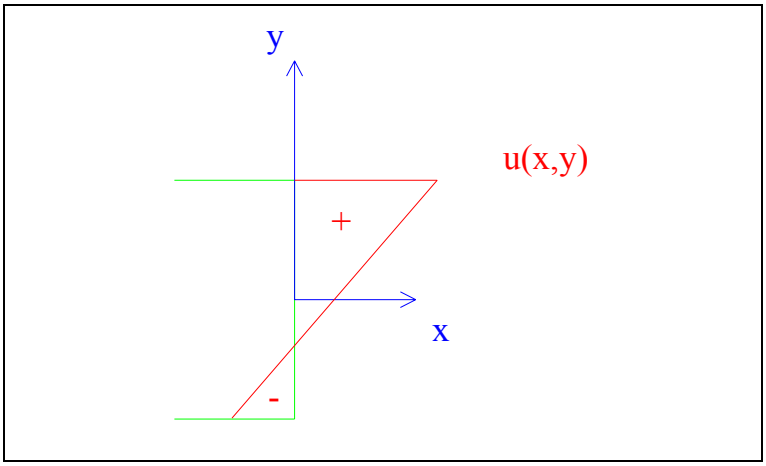

Figure 5.2 Stress sign criteria

Figure (5.2) shows the sign criteria used in equation (5.1). These kinematic considerations give us the expression for the plastic extension in the direction of axis x (longitudinal axis) at an arbitrary point of the plasticized cross section can be expressed by a linear function

$$e_p(y) = \frac{\partial u(x,y,x)}{\partial x} \tag{5.2}$$

$$e_p(y) = \frac{\partial u(x)}{\partial x} - y\frac{\partial^2 v(x)}{\partial x^2} \tag{5.3}$$

where y is the coordinate perpendicular to the bending axis. The plastic extension at $y=0$, $e_p(0) = \frac{\partial u(x)}{\partial x}$. Now the plastic dissipation can be expressed as,

$$D_{\text{int}} = \int_{l^e}\int_{A} \sigma(y) e_p(y) dA dx \tag{5.4}$$

If it is considered that $\sigma(y)\bar{e}_p(y) > 0$ for all y in the cross section, and that the absolute value of $\sigma(y)$ at the limit state is σ_y. Then the following equation for the plastic dissipation is obtained

$$D_{\text{int}} = \int_{l^e} \sigma_y \int_{A} \left| e_p(y) \right| dA dx \tag{5.5}$$

The problem now is reduced to integrate exactly the absolute value of a planar surface.

To take in account the effects of plastic bending and normal forces brings us to equation (5.5). This equation depends on the sort of cross section, and has to be integrated for each particular cross section. When only plastic bending has been considered, equation (5.5) has been trivial to integrate, and we have been able to change the cross section by only changing the plastic moment. Expression (5.5) has to be obtained for each kind of cross section.

Chapter 6. Continuous beam and frames under the combination of plastic bending and compression (or tension).

6.1 Introduction

We will follow now the method explained in chapter 3 for the case of the combination of plastic bending and compression (or tension). The reasoning developed in chapter 4 is completely valid in this new case. There are a few differences:

- We have three degrees of freedom per node (u_i, v_i, θ_i).

- The plastic extension combines bending and compression (or tension).

$$e_p = \frac{du(x)}{dx} - y\frac{d^2v(x)}{dx^2} \tag{6.1}$$

6.2 Discretisation

All remain the same for the displacement $v(x)$. The same interpolation and the same shape functions are kept. The difference is that now an interpolation for the longitudinal displacement (local axis) $u(x)$ has to be proposed. The proposed interpolation is linear

$$u(x) = b_1 x + b_0 \tag{6.2}$$

Now, (6.2) will be expressed in function of the nodal degrees of freedom (u_1, u_2).

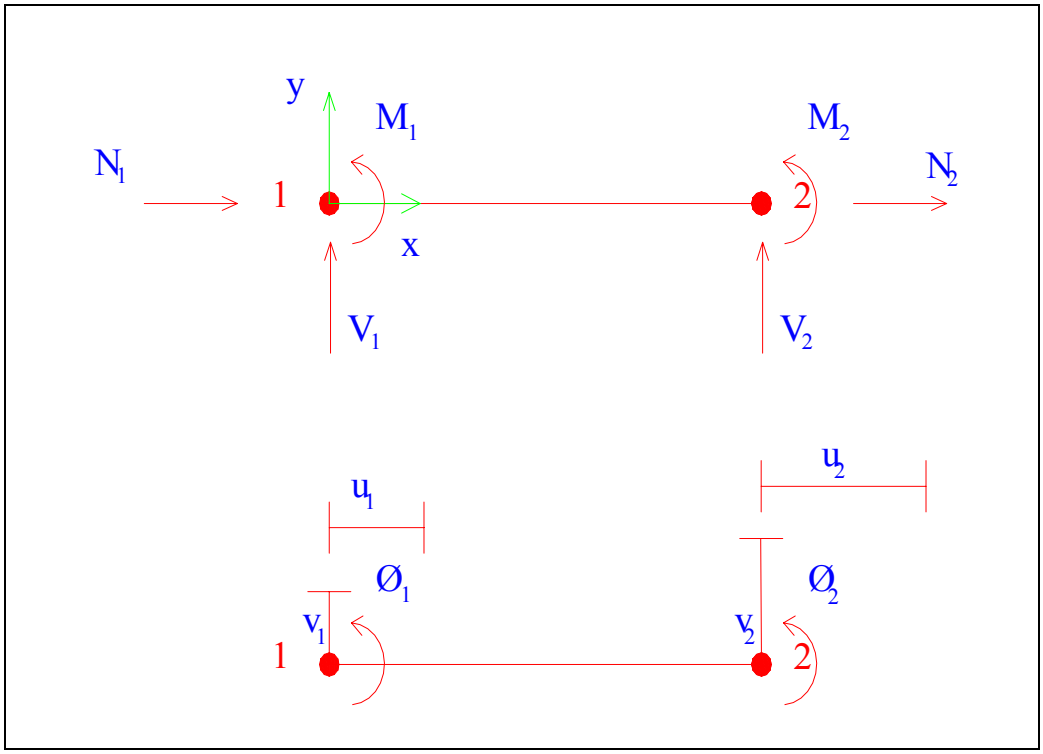

Figure 6.1 Nodal degrees of freedom and internal loads sign criteria.

In the same way as for *v(x)* in chapter 4, it easy to obtain the following expression for *u(x)*.

$$u(x) = N_5(x)u_1 + N_6(x)u_2 \tag{6.3}$$

where the functions $N_i(x)$ are the shape functions in this case. If l^e is the element length, then

$$N_5(x) = \frac{(l^e - x)}{l^e} \tag{6.4}$$

$$N_6(x) = \frac{x}{l^e} \tag{6.5}$$

Now this new degree of freedom is introduced into the matrix notation that has been defined in chapter 4. Similarly as equation (4.7) it can be defined

$$u(x) = [N_5(x) \quad 0 \quad 0 \quad N_6(x) \quad 0 \quad 0] \begin{bmatrix} u_1 \\ v_1 \\ \theta_1 \\ u_2 \\ v_2 \\ \theta_2 \end{bmatrix} = \mathbf{N}_u{}^T(x)\mathbf{v} \tag{6.6}$$

and equation (4.7), if this unified notation is considered, turns into

$$v(x) = [0 \quad N_1(x) \quad N_2(x) \quad 0 \quad N_3(x) \quad N_4(x)] \begin{bmatrix} u_1 \\ v_1 \\ \theta_1 \\ u_2 \\ v_2 \\ \theta_2 \end{bmatrix} = \mathbf{N}_v{}^T(x)\mathbf{v} \tag{6.7}$$

After having done all this adaptations the process follows exactly in the same way as in chapter 4.

6.3 Plastic element dissipation

Our aim in this section is to obtain the non-linear secant matrix for one element. Equation (6.8) give us the expression of the plastic dissipation for one element.

$$D^e_{\text{int}} = \int_{l^e}\int_{A} \sigma_y \left(\frac{du(x)}{dx} - y\frac{d^2v(x)}{dx^2}\right) dA dx \tag{6.8}$$

Let's use now the hypothesis that the tension has the same sign that the plastic extension. Then, the expression (6.8) turns into

$$D_{\text{int}}^{e} = \int_{l^e} \sigma_y \int_{A} \left| \frac{du(x)}{dx} - y\frac{d^2v(x)}{dx^2} \right| dAdx \tag{6.9}$$

Consider the following expressions

$$\frac{du(x)}{dx} = \frac{d}{dx}(\mathbf{N}_u^T(x)\mathbf{v}^e) = \frac{d}{dx}(\mathbf{N}_u^T(x))\mathbf{v}^e = \mathbf{B}_u^T(x)\mathbf{v}^e \tag{6.10}$$

$$\frac{d^2v(x)}{dx^2} = \frac{d^2}{dx^2}(\mathbf{N}_v^T(x)\mathbf{v}^e) = \frac{d^2}{dx^2}(\mathbf{N}_v^T(x))\mathbf{v}^e = \mathbf{B}_v^T(x)\mathbf{v}^e \tag{6.11}$$

expression (6.9) can be expressed as

$$D_{\text{int}}^{e} = \int_{l^e} \sigma_y \int_{A} \left| \mathbf{B}_u^T\mathbf{v}^e - y\mathbf{B}_v^T\mathbf{v}^e \right| dAdx \tag{6.12}$$

where, whether l^e is the length of the element

$$\mathbf{B}_u = \begin{bmatrix} -\frac{1}{l^e} \\ 0 \\ 0 \\ \frac{1}{l^e} \\ 0 \\ 0 \end{bmatrix} \quad \text{and} \quad \mathbf{B}_v = \begin{bmatrix} 0 \\ \frac{d^2N_1}{dx^2} \\ \frac{d^2N_2}{dx^2} \\ 0 \\ \frac{d^2N_3}{dx^2} \\ \frac{d^2N_4}{dx^2} \end{bmatrix}(x) \tag{6.13}$$

In our mesh it is considered that the elements are fully plastizised. Therefore, it can be written

$$D_{\text{int}}^{e} = \sigma_y \int_{l^e} \int_{A} \left| \mathbf{B}_u^T\mathbf{v}^e - y\mathbf{B}_v^T\mathbf{v}^e \right| dAdx \tag{6.14}$$

Note that it is considered that the element has constant limit elastic in order to simplify the integral.

Our problem now is how integrate (6.14). The integration along the element will be carried out by using the same numerical integration described in chapter 4. The surface integral described by (6.14) it is the integral of the absolute value of a planar surface. This can be easily exactly integrated if we know the point where the line changes its sign. This is when

$$e_p(y) = 0 \tag{6.15}$$

using the equation (6.1), the coordinate *y* that we are looking for is

$$\bar{y} = \frac{\mathbf{B}_u^T \mathbf{v}^e}{\mathbf{B}_v^T \mathbf{v}^e} \tag{6.16}$$

We want to reach an unique expression for the plastic dissipation. There are two cases to integrate. The case when $\bar{y}$ does not belong to the cross section and the case when it does. An expression capable to simulate these two situations with continuity is needed.

Equation (6.14) it is easy to obtain for a rectangular cross section. It is reduced to the integration of a simple line. You just have to multiply the value of the line at the centroid of its domain by the area of its domain. If the cross section is not rectangular you can approximate the domain by rectangular sections and then integrate as explained before.

The procedure explained before uses one point per domain to integrate the absolute value of a line. You have to notice that if only one point is used the expression, that is obtained for the cases where $\bar{y}$ does not belong to the cross section, cannot simulate bending in double symmetric cross sections. When the case before mentioned is considered, expression (6.12) is

$$D_{\text{int}}^e = \int_{l^e} \sigma_y A e_p(0) dx = \int_{l^e} \sigma_y A \left| \mathbf{B}_u^T \mathbf{v}^e \right| dx \tag{6.17}$$

and therefore, the term of bending does not appear. This problem can be easily solved if two points of integration are considered. Gauss-Legendre quadrature of two points of integration or to propose our own points of integration can be used, with both the same result will be reached.

Let's concentrate in two specific cross sections: rectangular cross section and a double T cross section.

6.4 Plastic element dissipation. Rectangular cross section.

Consider a rectangular cross section with height *h* and width *b*. Equation (6.12) is

$$D_{\text{int}}^e = \sigma_y b \int_{l^e} \int_{-\frac{h}{2}}^{\frac{h}{2}} \left| \mathbf{B}_u^T \mathbf{v}^e - y \mathbf{B}_v^T \mathbf{v}^e \right| dy dx \tag{6.18}$$

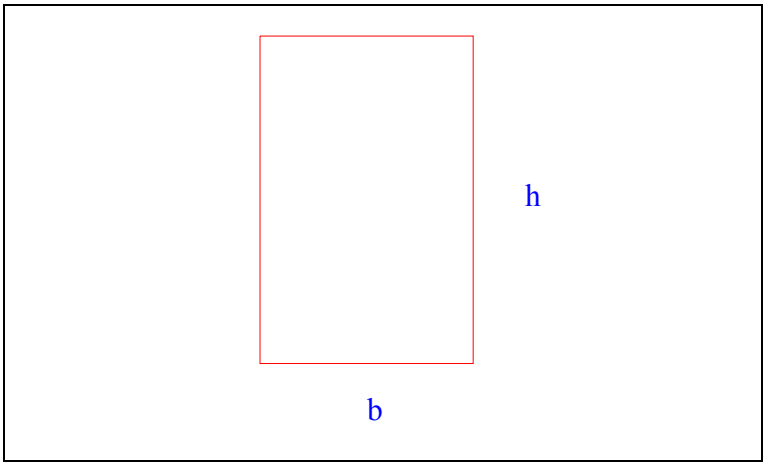

Figure 6.2 Rectangular cross section

The integration points considered for coordinate y are,

$$y_1 = \frac{1}{4}\cdot\frac{\mathbf{B}_u^T\mathbf{v}^e}{\mathbf{B}_v^T\mathbf{v}^e} + \frac{3}{4}\cdot\frac{h}{2} \tag{6.19}$$

$$y_2 = \frac{3}{4}\cdot\frac{\mathbf{B}_u^T\mathbf{v}^e}{\mathbf{B}_v^T\mathbf{v}^e} + \frac{1}{4}\cdot\frac{h}{2} \tag{6.20}$$

$$y_3 = \frac{3}{4}\cdot\frac{\mathbf{B}_u^T\mathbf{v}^e}{\mathbf{B}_v^T\mathbf{v}^e} - \frac{1}{4}\cdot\frac{h}{2} \tag{6.21}$$

$$y_4 = \frac{1}{4}\cdot\frac{\mathbf{B}_u^T\mathbf{v}^e}{\mathbf{B}_v^T\mathbf{v}^e} - \frac{3}{4}\cdot\frac{h}{2} \tag{6.22}$$

Each of these coordinates has associated one plastic extension. We will denote e_i the plastic extension associated to y_i. An expression for equation (6.18) can be obtained.

$$D_{\text{int}}^e = \frac{\sigma_y b}{2}\int_{l^e}\left[\left(\frac{h}{2} - \frac{\mathbf{B}_u^T\mathbf{v}^e}{\mathbf{B}_v^T\mathbf{v}^e}\right)\left(|e_1| + |e_2|\right) + \left(\frac{h}{2} + \frac{\mathbf{B}_u^T\mathbf{v}^e}{\mathbf{B}_v^T\mathbf{v}^e}\right)\left(|e_3| + |e_4|\right)\right]dx \tag{6.23}$$

Equation (6.23) not only give us the expression for the plastic dissipation but also give us an easy way to find the secant matrix of the non-linear system that has to be solved. Equation (6.23) is now

$$D_{\text{int}}^e = \frac{\sigma_y b}{2}\int_{l^e}\left[\left(\frac{h}{2} - \frac{\mathbf{B}_u^T\mathbf{v}^e}{\mathbf{B}_v^T\mathbf{v}^e}\right)\left(\frac{|e_1|^2}{|e_1|} + \frac{|e_2|^2}{|e_2|}\right) + \left(\frac{h}{2} + \frac{\mathbf{B}_u^T\mathbf{v}^e}{\mathbf{B}_v^T\mathbf{v}^e}\right)\left(\frac{|e_3|^2}{|e_3|} + \frac{|e_4|^2}{|e_4|}\right)\right]dx \tag{6.24}$$

On the other hand,

$$|e_i|^2 = (\mathbf{B}_u^T\mathbf{v}^e - y_i\mathbf{B}_v^T\mathbf{v}^e)\cdot(\mathbf{B}_u^T\mathbf{v}^e - y_i\mathbf{B}_v^T\mathbf{v}^e) = ((\mathbf{B}_u^T - y_i\mathbf{B}_v^T)\mathbf{v}^e)\cdot((\mathbf{B}_u^T - y_i\mathbf{B}_v^T)\mathbf{v}^e) =$$

$$= (\mathbf{v}^{eT}(\mathbf{B}_u - y_i\mathbf{B}_v))\cdot((\mathbf{B}_u^T - y_i\mathbf{B}_v^T)\mathbf{v}^e) =$$

$$= \mathbf{v}^{eT}(\mathbf{B}_u - y_i\mathbf{B}_v)\cdot(\mathbf{B}_u^T - y_i\mathbf{B}_v^T)\mathbf{v}^e = \mathbf{v}^{eT}\mathbf{k}_i\mathbf{v}^e \tag{6.25}$$

where

$$\mathbf{k}_i = \mathbf{B}_u\mathbf{B}_u^T - y_i(\mathbf{B}_v\mathbf{B}_u^T + \mathbf{B}_u\mathbf{B}_v^T) + y_i^2\mathbf{B}_v\mathbf{B}_v^T \tag{6.26}$$

therefore a secant matrix $\mathbf{k}_s$ expressed per unit of length can be found. This matrix will be integrated along the length of the element with a Gauss-Legendre quadrature.

$$\mathbf{k}_s = \frac{\sigma_y b}{2}a\left[(\frac{1}{|e_1|}+\frac{1}{|e_2|})\mathbf{B}_u\mathbf{B}_u^T - (\frac{y_1}{|e_1|}+\frac{y_2}{|e_2|})(\mathbf{B}_v\mathbf{B}_u^T + \mathbf{B}_u\mathbf{B}_v^T) + (\frac{y_1^2}{|e_1|}+\frac{y_2^2}{|e_2|})\mathbf{B}_v\mathbf{B}_v^T\right] +$$

$$+\frac{\sigma_y b}{2}c\left[(\frac{1}{|e_3|}+\frac{1}{|e_4|})\mathbf{B}_u\mathbf{B}_u^T - (\frac{y_3}{|e_3|}+\frac{y_4}{|e_4|})(\mathbf{B}_v\mathbf{B}_u^T + \mathbf{B}_u\mathbf{B}_v^T) + (\frac{y_3^2}{|e_3|}+\frac{y_4^2}{|e_4|})\mathbf{B}_v\mathbf{B}_v^T\right] \tag{6.27}$$

where

$$a = (\frac{h}{2} - \frac{\mathbf{B}_u^T\mathbf{v}^e}{\mathbf{B}_v^T\mathbf{v}^e}) \tag{6.28}$$

$$c = (\frac{h}{2} + \frac{\mathbf{B}_u^T\mathbf{v}^e}{\mathbf{B}_v^T\mathbf{v}^e}) \tag{6.29}$$

$$\mathbf{B}_u\mathbf{B}_u^T = \begin{bmatrix} \frac{1}{l^{e2}} & 0 & 0 & -\frac{1}{l^{e2}} & 0 & 0 \\ 0 & 0 & 0 & 0 & 0 & 0 \\ 0 & 0 & 0 & 0 & 0 & 0 \\ -\frac{1}{l^{e2}} & 0 & 0 & \frac{1}{l^{e2}} & 0 & 0 \\ 0 & 0 & 0 & 0 & 0 & 0 \\ 0 & 0 & 0 & 0 & 0 & 0 \end{bmatrix} \tag{6.30}$$

$$\mathbf{B}_v\mathbf{B}_v^T = \begin{bmatrix} 0 & 0 & 0 & 0 & 0 & 0 \\ 0 & \frac{d^2N_1}{dx^2}\frac{d^2N_1}{dx^2} & \frac{d^2N_1}{dx^2}\frac{d^2N_2}{dx^2} & 0 & \frac{d^2N_1}{dx^2}\frac{d^2N_3}{dx^2} & \frac{d^2N_1}{dx^2}\frac{d^2N_4}{dx^2} \\ 0 & \frac{d^2N_2}{dx^2}\frac{d^2N_1}{dx^2} & \frac{d^2N_2}{dx^2}\frac{d^2N_2}{dx^2} & 0 & \frac{d^2N_2}{dx^2}\frac{d^2N_3}{dx^2} & \frac{d^2N_2}{dx^2}\frac{d^2N_4}{dx^2} \\ 0 & 0 & 0 & 0 & 0 & 0 \\ 0 & \frac{d^2N_3}{dx^2}\frac{d^2N_1}{dx^2} & \frac{d^2N_3}{dx^2}\frac{d^2N_2}{dx^2} & 0 & \frac{d^2N_3}{dx^2}\frac{d^2N_3}{dx^2} & \frac{d^2N_3}{dx^2}\frac{d^2N_4}{dx^2} \\ 0 & \frac{d^2N_4}{dx^2}\frac{d^2N_1}{dx^2} & \frac{d^2N_4}{dx^2}\frac{d^2N_2}{dx^2} & 0 & \frac{d^2N_4}{dx^2}\frac{d^2N_3}{dx^2} & \frac{d^2N_4}{dx^2}\frac{d^2N_4}{dx^2} \end{bmatrix} \tag{6.31}$$

$$\mathbf{B}_u\mathbf{B}_v^T = \begin{bmatrix} 0 & -\frac{1}{l^e}\frac{d^2N_1}{dx^2} & -\frac{1}{l^e}\frac{d^2N_2}{dx^2} & 0 & -\frac{1}{l^e}\frac{d^2N_3}{dx^2} & -\frac{1}{l^e}\frac{d^2N_4}{dx^2} \\ 0 & 0 & 0 & 0 & 0 & 0 \\ 0 & 0 & 0 & 0 & 0 & 0 \\ 0 & \frac{1}{l^e}\frac{d^2N_1}{dx^2} & \frac{1}{l^e}\frac{d^2N_2}{dx^2} & 0 & \frac{1}{l^e}\frac{d^2N_3}{dx^2} & \frac{1}{l^e}\frac{d^2N_4}{dx^2} \\ 0 & 0 & 0 & 0 & 0 & 0 \\ 0 & 0 & 0 & 0 & 0 & 0 \end{bmatrix} \tag{6.32}$$

Note that the following condition must be imposed,

$$\text{If } \frac{\mathbf{B}_u^T\mathbf{v}^e}{\mathbf{B}_v^T\mathbf{v}^e} \geq \frac{h}{2} \text{ then } \frac{\mathbf{B}_u^T\mathbf{v}^e}{\mathbf{B}_v^T\mathbf{v}^e} = \frac{h}{2}$$

$$\text{If } \frac{\mathbf{B}_u^T\mathbf{v}^e}{\mathbf{B}_v^T\mathbf{v}^e} \leq -\frac{h}{2} \text{ then } \frac{\mathbf{B}_u^T\mathbf{v}^e}{\mathbf{B}_v^T\mathbf{v}^e} = -\frac{h}{2}$$

With these two conditions continuity in the matrix $\mathbf{k}_s$ is assured.

6.5 Plastic element dissipation. Double T cross section.

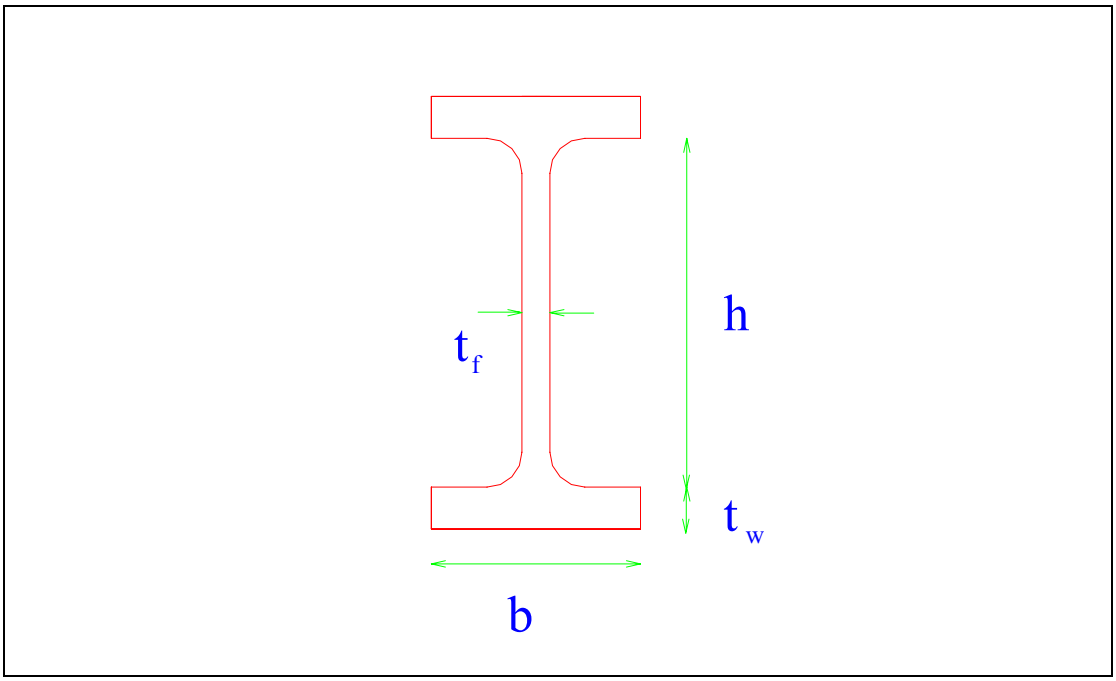

Figure 6.3 Double T cross section

Figure (6.3) shows a double T cross section. For structural purposes it can be supposed that the wings have the same coordinate *y* in all their width. This simplifies the evaluation of the integral (6.12). Under this supposition (6.12) can be expressed as

$$D_{\text{int}}^{e} = \sigma_y b t_f \int_{l^e} \left(\left| \mathbf{B}_u^T \mathbf{v}^e - \frac{h}{2} \mathbf{B}_v^T \mathbf{v}^e \right| + \left| \mathbf{B}_u^T \mathbf{v}^e + \frac{h}{2} \mathbf{B}_v^T \mathbf{v}^e \right| \right) dx +$$

$$+ \sigma_y t_w \int_{l^e} \int_{-\frac{h}{2}}^{\frac{h}{2}} | \mathbf{B}_u^T \mathbf{v}^e - y \mathbf{B}_v^T \mathbf{v}^e | dy dx \tag{6.33}$$

The last term of the addition has the same structure than the rectangular cross section. And we will integrate it using the same four points we have used for the rectangular cross section. The double T cross section has two additional terms related to the wings. Again, it is easy to find the contribution of the wings to the secant matrix. Following a similar reasoning than before, expression (6.32) is obtained for the secant matrix per unit of length for a double T cross section (Double symmetric). If the same denotation as the rectangular cross section is kept, and consider the following extensions

$$e_5 = \mathbf{B}_u^T \mathbf{v}^e - \frac{h}{2} \mathbf{B}_v^T \mathbf{v}^e \tag{6.34}$$

$$e_6 = \mathbf{B}_u^T \mathbf{v}^e + \frac{h}{2} \mathbf{B}_v^T \mathbf{v}^e \tag{6.35}$$

the secant matrix for one cross section per unit of length is

$$\mathbf{k}_s = \frac{\sigma_y t_w}{2} a \left[\left(\frac{1}{|e_1|} + \frac{1}{|e_2|} \right) \mathbf{B}_u \mathbf{B}_u^T - \left(\frac{y_1}{|e_1|} + \frac{y_2}{|e_2|} \right) (\mathbf{B}_v \mathbf{B}_u^T + \mathbf{B}_u \mathbf{B}_v^T) + \left(\frac{y_1^2}{|e_1|} + \frac{y_2^2}{|e_2|} \right) \mathbf{B}_v \mathbf{B}_v^T \right] +$$

$$+ \frac{\sigma_y t_w}{2} c \left[\left(\frac{1}{|e_3|} + \frac{1}{|e_4|} \right) \mathbf{B}_u \mathbf{B}_u^T - \left(\frac{y_3}{|e_3|} + \frac{y_4}{|e_4|} \right) (\mathbf{B}_v \mathbf{B}_u^T + \mathbf{B}_u \mathbf{B}_v^T) + \left(\frac{y_3^2}{|e_3|} + \frac{y_4^2}{|e_4|} \right) \mathbf{B}_v \mathbf{B}_v^T \right] +$$

$$+ \frac{\sigma_y b t_f}{2} \left[\left(\frac{1}{|e_5|} + \frac{1}{|e_6|} \right) \mathbf{B}_u \mathbf{B}_u^T - \frac{h}{2} \left(\frac{1}{|e_5|} - \frac{1}{|e_6|} \right) (\mathbf{B}_v \mathbf{B}_u^T + \mathbf{B}_u \mathbf{B}_v^T) + \frac{h^2}{4} \left(\frac{1}{|e_5|} + \frac{1}{|e_6|} \right) \mathbf{B}_v \mathbf{B}_v^T \right] \tag{6.36}$$

where

$$a = \left(\frac{h}{2} - \frac{\mathbf{B}_u^T \mathbf{v}^e}{\mathbf{B}_v^T \mathbf{v}^e} \right) \tag{6.37}$$

$$c = \left(\frac{h}{2} + \frac{\mathbf{B}_u^T \mathbf{v}^e}{\mathbf{B}_v^T \mathbf{v}^e} \right) \tag{6.38}$$

Matrix (6.36) will be integrated along the element using a two points Gauss-Legendre quadrature.

If you consider now another kind of cross section you can obtain the secant matrix dividing it in rectangular sections and integrating them using the method before

explained. The procedure is then: first, find the value of $\bar{y}$ and then integrate each rectangular section separately. The accuracy will depend on the quality of the approximation to the real cross section.

6.6 External loads work.

The only difference with the case of pure plastic bending is that now the effect of the normal component N and t_x (distributed load) are introduced. The expression of the external work is,

$$W_{ext}^{e} = \int_{l^e} t_y^e(x)\, v\ (x)\, dS + \int_{l^e} t_x^e(x)\, u\ (x)\, dS + \sum_i^n F_i^e\, v(x_i) + \sum_i^m N_i^e\, u(x_i) + \sum_i^k M_i^e\, \theta(x_i) \tag{6.39}$$

where $t_x(x)$ represent the distributed loads in the direction of displacement u, $t_y(x)$ represent the distributed loads in the direction of displacement v, F_i represent the point loads in the x_i points, N_i are the point normal loads in the x_i points and M_i are the point moments in the x_i points. To obtain a simplified integral it is considered that within one element the distributed loads do not change with x. Equation (6.39) allows us to easily consider distributed loads.

As in chapter 4 expression (6.39) can be expressed in matrix notation. In analogy with (4.20) the external work for one element can be expressed in function of the load multiplier as,

$$W_{ext}^{e} = \mu_k [(\hat{\mathbf{F}}_1^{t_x\,T} + \hat{\mathbf{F}}_1^{t_y\,T} + \hat{\mathbf{F}}_1^{F\,T} + \hat{\mathbf{F}}_1^{N\,T} + \hat{\mathbf{F}}_1^{M\,T}) \quad (\hat{\mathbf{F}}_2^{t_x\,T} + \hat{\mathbf{F}}_2^{t_y\,T} + \hat{\mathbf{F}}_2^{F\,T} + \hat{\mathbf{F}}_2^{N\,T} + \hat{\mathbf{F}}_2^{M\,T})] \begin{bmatrix} \mathbf{v}_1^e \\ \mathbf{v}_2^e \end{bmatrix}$$

$$= [\hat{\mathbf{F}}_1^{e\,T} \quad \hat{\mathbf{F}}_2^{e\,T}]\mathbf{v} \begin{bmatrix} \mathbf{v}_1^e \\ \mathbf{v}_2^e \end{bmatrix} = \mu_k \hat{\mathbf{f}}^{e\,T} \mathbf{v}^e = \mu_k \hat{W}_{ext}^{e} \tag{6.40}$$

Then the total external work in the structure is

$$W_{ext} = \mu_k \sum_e \hat{W}_{ext}^{e} = \mu_k \hat{W}_{ext} \tag{6.41}$$

Our variables are once again the multiplier μ_k and the nodal degrees of freedom (u_i, v_i, θ_i).

Once at this point, the global stiffness matrix is assembled as in the standard stiffness methods. The optimization problem is solve as explained in chapter 4.

The program that we join with this work develops the method exposed in the more general case of combination of plastic bending and tension (or compression). It uses some subroutines of the program Lingflag developed by Javier Bonet. Our program contains step by step explanations of all the subroutines. We have considered useless to describe all the program in this pages.

6.7 Examples

The goal of this section is to illustrate with examples how the method performs for the case of combination of plastic bending and tension (or compression). First, it is presented present two trivial examples. Finally, we will focus on more complicated examples.

In all the examples, convergence has been achieved with seven significant figures. And the parameter ε, that is introduced to avoid dividing by zero, is 10^{-5}.

Example 1

Section properties:

Rectangular cross section:
h =0,1 m
b= 0,05 m

Limit elastic: $\sigma_y = 275000000 \ \ Pa$

Plastic moment: $M_p = \frac{bh^2\sigma_y}{4} = 34375 \ \ Nm$

Plastic normal force: $N=bh\sigma_y=1375000\ N$

Consider the loaded beam of figure 6.4.

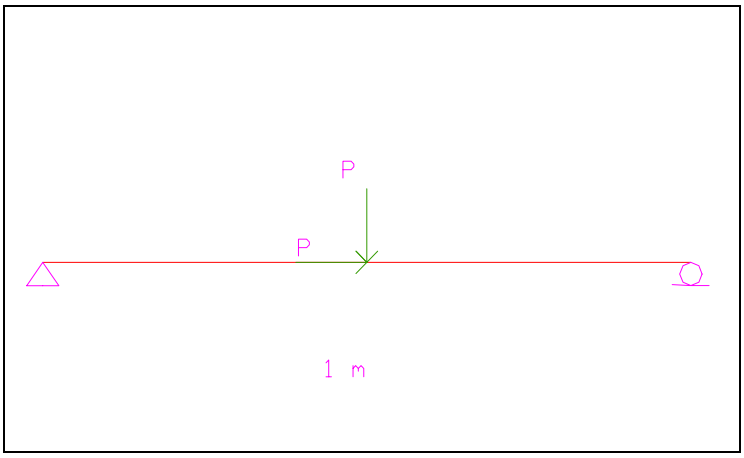

Figure 6.4 1-Span beam

Figures 6.5 and 6.6 show the real mechanism of collapse and the one is found when running the program. You can observe that the expected behavior is obtained. The elements concentrate where the plastic hinge appears: the mid cross section.

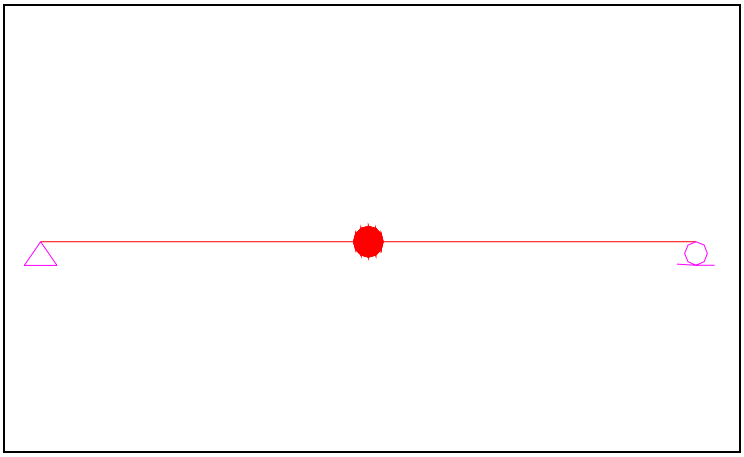

Figure 6.5 Mechanism of collapse

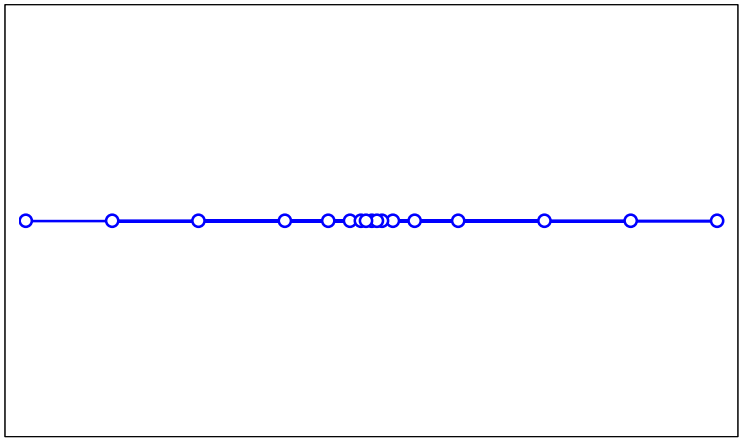

Figure 6.6 Mesh 14 elements

It is easy to find the real collapse load of this structure under these loads. You just have to introduce the equation of the plastic envelope for a rectangular cross section into the equilibrium equations. The real collapse load is 137157,9581 N. In figure 6.7 and table 6.1 it is shown the sequence of upper and lower bound in the case of a considered very fine mesh of 128 elements. Your can note that, the lower bounds are bigger that the real collapse load. This reflects once again that the reference mesh considered at the beginning is not fine enough.

Another important observation is that the lower bound remains constant as the mesh is refined. The difference between this example and the others is that this one is isostatic. It seems that the fact of being isostatic is enough to warranty it. To prove this fact is not the aim of this paper, but it may be considered in future papers.

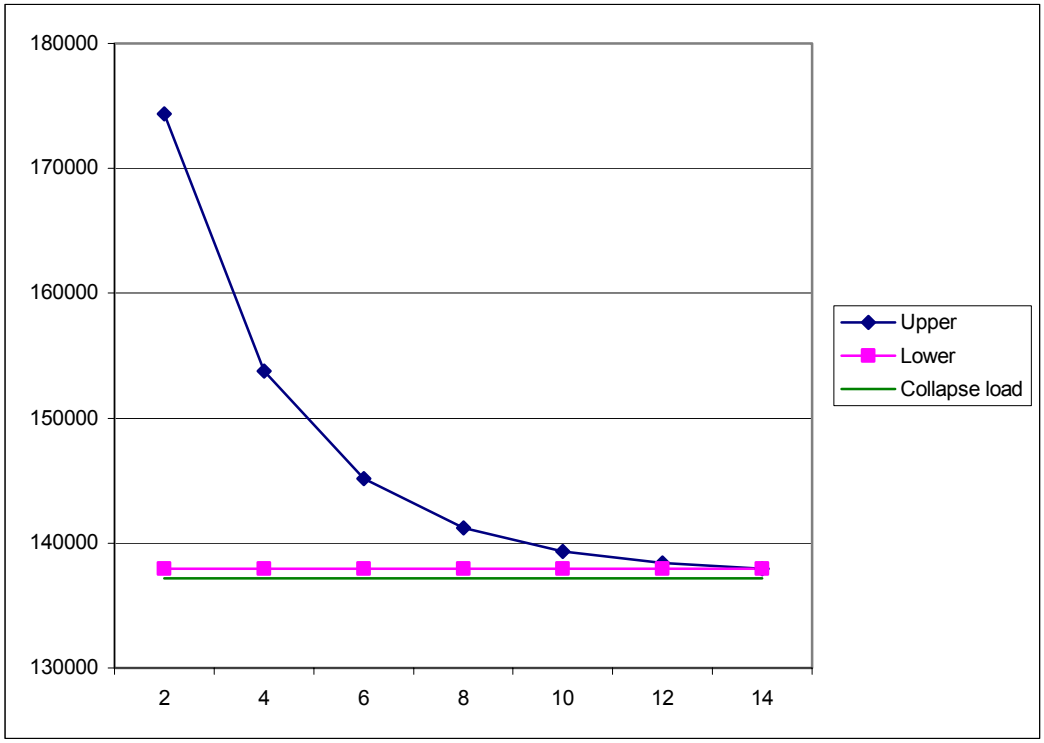

Figure 6.7 Sequence of Upper and Lower bounds

number of elements	Upper bound (N)	Lower bound (N)
2	174343	137954
4	153745	137954
6	145169	137954
8	141230	137954
10	139340	137954
12	138416	137954
14	137958	137954

Table 6.1 Upper bound and Lower bound

Example 2

Section properties:

Rectangular cross section:
h =0,125 m
b= 0,05 m

Limit elastic: $\sigma_y = 275000000 \ \ Pa$

Plastic moment: $M_p = \frac{bh^2\sigma_y}{4} = 34375 \ \ Nm$

Plastic normal force: $N=bh\sigma_y=1375000\ N$

Let's consider the structure in figure 6.8. We have taken this example from Milan Jirásek and ZdeneK P. Bazant (2001). They have proposed another method to obtain

the collapse load of the structure. They have found that the collapse load is approximately $P = 2{,}303\frac{M_p}{L}$. In our case $L = 1\ m$ and $M_p = 123696{,}28\ Nm$. Therefore, the collapse load is $P = 123969{,}28\ N$.

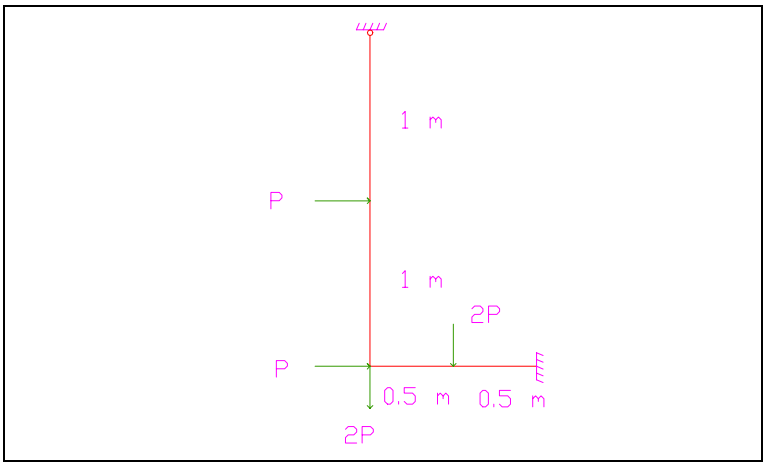

Figure 6.8 Structure example 2

The mechanism of collapse is shown in figures 6.9 and 6.10. Your can see that the model obtained matches the expected mechanism of collapse. In Figure 6.10 it has been represented a mesh of 28.

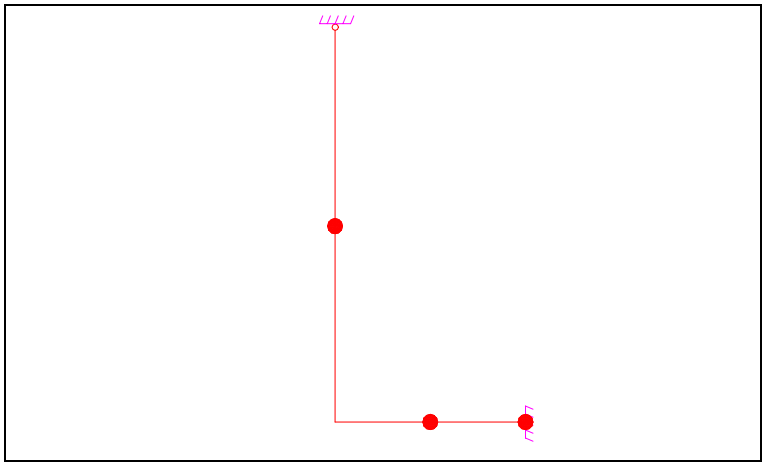

Figure 6.9 Mechanism of collapse

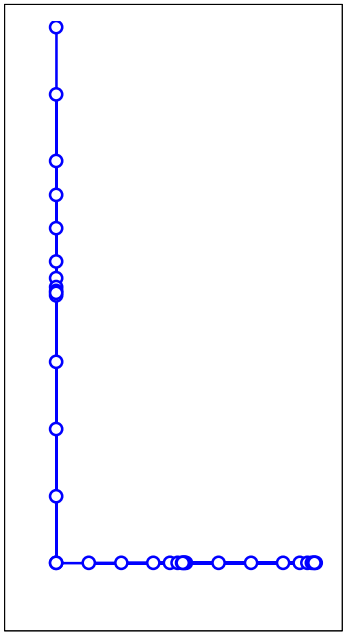

Figure 6.10 Mesh 22 elements

The sequence of upper and lower bounds is shown in figure 6.11 and table 6.2. This values have been obtained supposing a reference mesh of 1024 elements. The results obtained have been compared with the real collapse load. You can observe that the values, that have been found, are an upper bound of the collapse load.

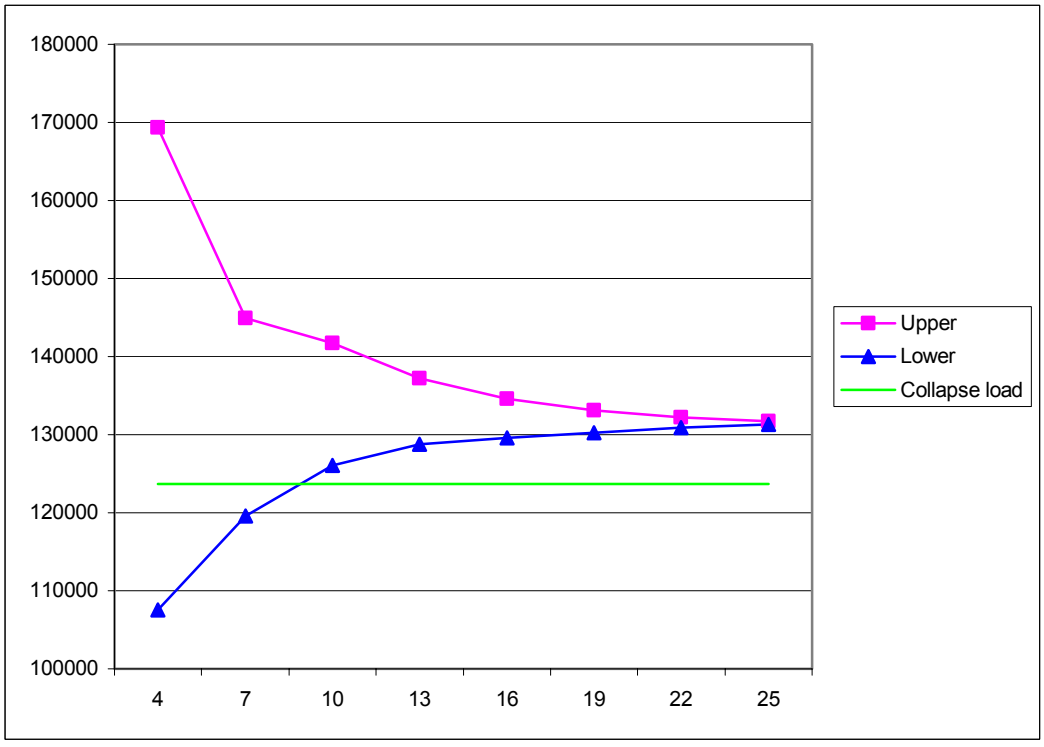

Figure 6.11 Upper bound and Lower bound convergence.

Number of elements	*Upper bound (N)*	*Lower bound (N)*
4	169319	107565
7	144955	119614
10	141725	126043
13	137224	128738
16	134566	129630
19	133078	130234
22	132218	130876
25	131758	131290

Table 6.2 Upper bound and Lower bound

Example 3

Section properties:

Rectangular cross section:
h =0,1 m
b= 0,05 m
Limit elastic: $\sigma_y = 275000000 \ \ Pa$

Plastic moment: $M_p = \frac{bh^2\sigma_y}{4} = 34375 \ \ Nm$

Plastic normal force: $N=bh\sigma_y=1375000\ N$

It has been found a sequence of lower and upper bounds for the example shown in figure 6.12. Lynn S. Beedle (1958) treated this specific case in the past. He found that the collapse load when only pure plastic bending is taken into account is $P = \frac{9M_p}{11L}$. In our case $L=1\ m$. This makes that $P= 28125\ N$.

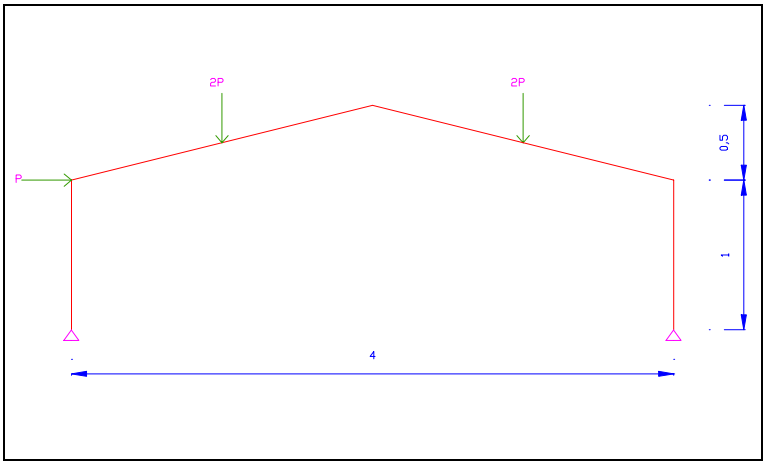

Figure 6.12 Structure example 3

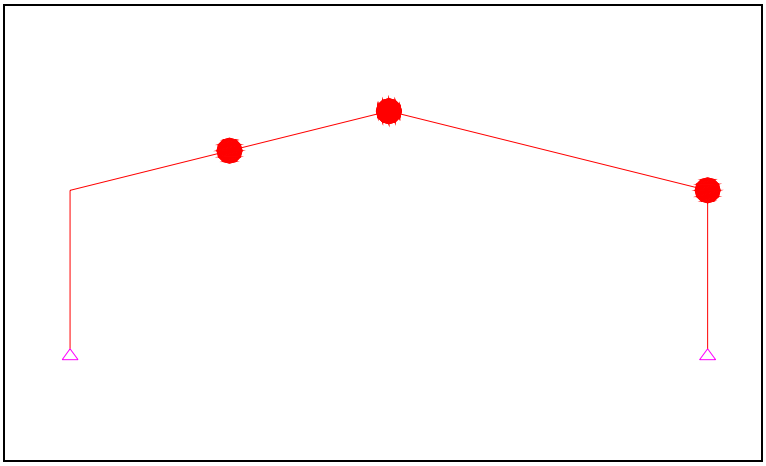

Figure 6.13 Mechanism of collapse

Figure 6.14 show how the elements concentrate around the cross sections where plastic hinges are supposed to appear.

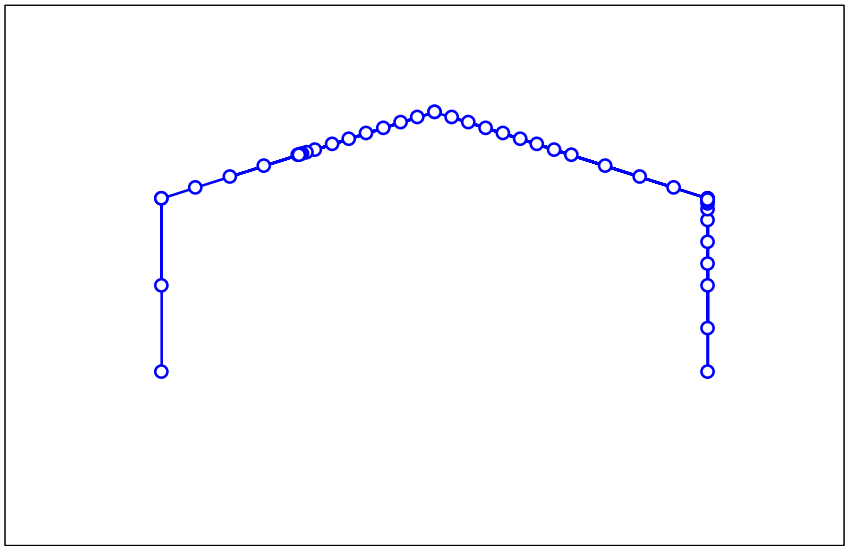

Figure 6.14 Mesh 65 elements

Figure 6.15 and table 6.3 show us the convergence of the upper and lower bounds for an initial supposed fine mesh of 192 elements. It has been added the collapse load when pure plastic bending alone is considered. In this case the collapse load towards the bounds are converging is bigger than the collapse load you obtain only considering pure plastic bending. If we consider a initial supposed mesh of 768 elements, the value towards the bounds are converging is between *28266 N* and *28113 N*. In this case the collapse load in pure plastic bending is between these values.

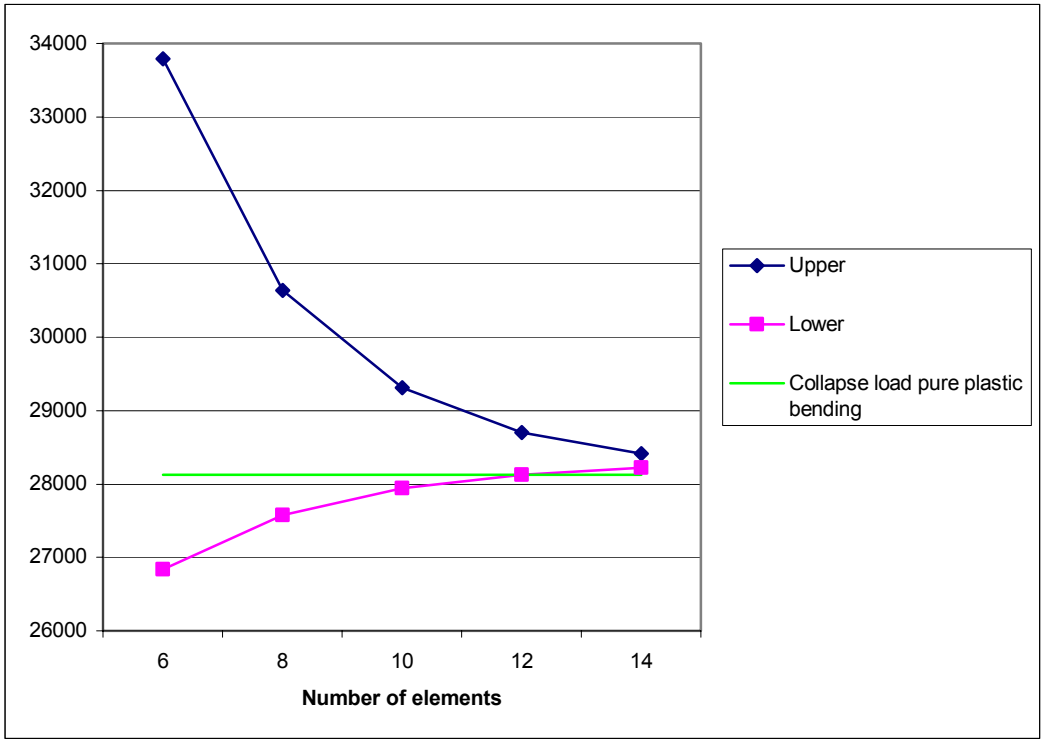

Figure 6.15 Upper bound and Lower bound convergence.

number of elements	*Upper bound (N)*	*Lower bound (N)*
6	33798	26833
8	30634	27579
10	29311	27947
12	28702	28130
14	28410	28221

Table 6.3 Upper and Lower bounds convergence.

Example 4

Section properties:

Rectangular cross section:
h =0,1 m
b= 0,05 m

Limit elastic: $\sigma_y = 275000000 \ \ Pa$

Plastic moment: $M_p = \frac{bh^2\sigma_y}{4} = 34375 \ \ Nm$

Plastic normal force: $N=bh\sigma_y=1375000\ N$

For example 4, J. Chakrabarty (1987) found the value of the collapse load when only perfect plastic bending is taken into account. This value is $P = \frac{32M_p}{17L}$. In our case $L=1\ m$, then the collapse load is $P= 64705\ N$.

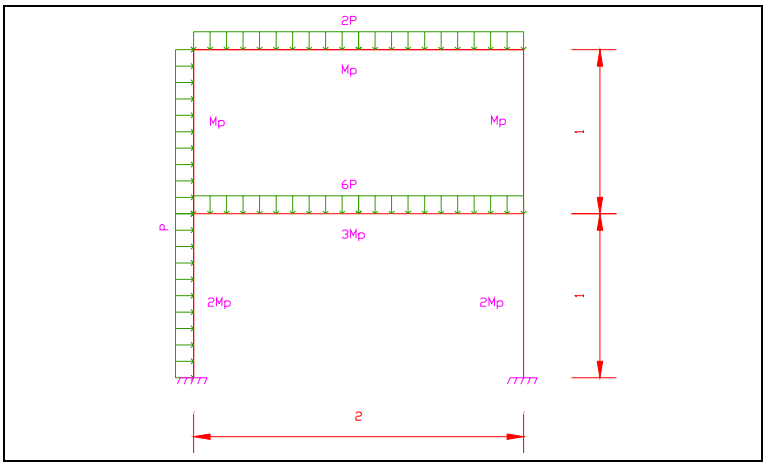

Figure 6.16 Structure example 4.

The distributed loads make difficult to foresee where the plastic hinges will appear. Figure 6.18 shows the mesh obtained when solving the problem.

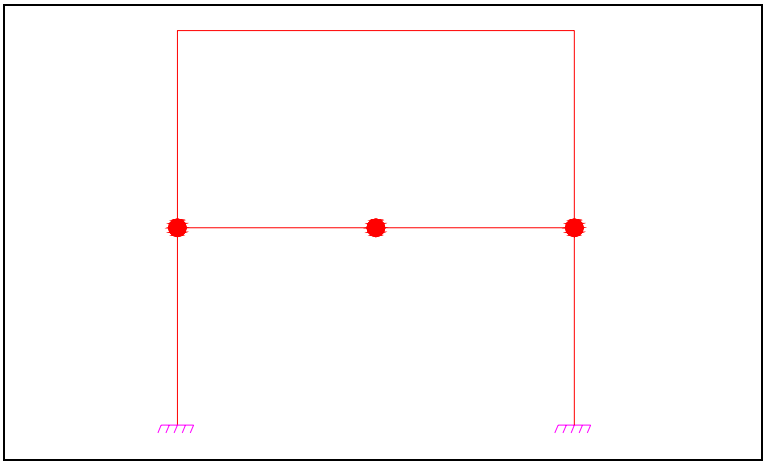

Figure 6.17 Mechanism of collapse

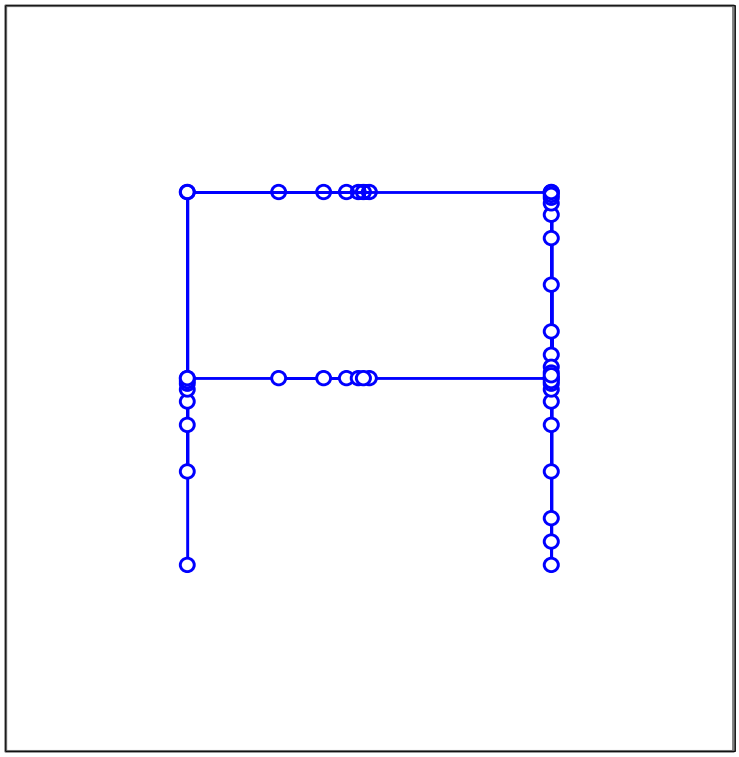

Figure 6.18 Mechanism of collapse

In figure 6.19 and table 6.4 it seems that the collapse load towards which the bounds are converging is the collapse load when we do not consider the effect of normal forces. These values have been found starting with a mesh of 6 elements until a mesh of 31 elements. It has been considered that the very reference mesh has 192 elements. If a reference mesh of 384 elements is considered, we obtain as the last values *64648 N (Upper)* and *63794 N (Lower)*. The collapse load when considering only plastic bending is then bigger than the last upper value found. If we continue improving the initial supposed reference mesh, these values would differ even more.

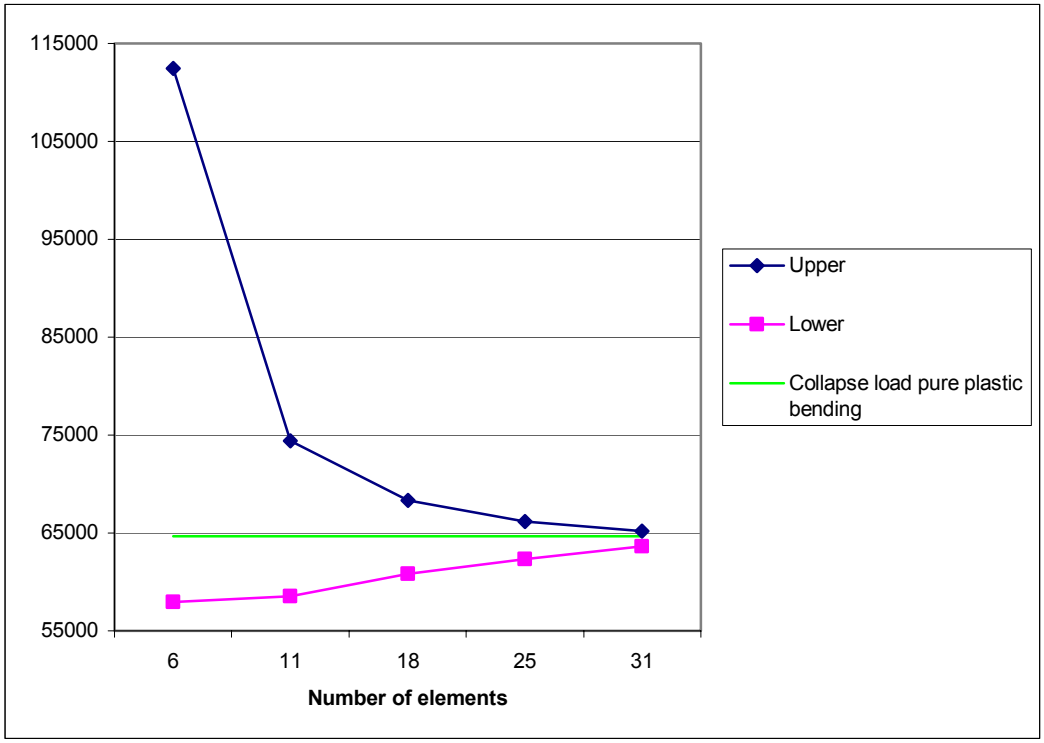

Figure 6.19 Sequence of Upper and Lower bounds.

Number of elements	*Upper bound (N)*	*Lower bound (N)*
6	112438	57970
11	74397	60077
18	68340	60027
25	66205	61495
31	65193	62806
37	64648	63794

Table 6.4 Upper and Lower bounds.

Chapter 7. Conclusions and recommendations

In this work, it has been exposed a method to work out the upper bound and the lower bound of the collapse load of a planar bar structure made of a perfect plastic material. We have concentrated in two cases: pure plastic bending and combination of plastic bending and tension (or compression). It has been shown that it is possible to find a sequence of upper and lower bounds that converge to one specific value trough a refinement process.

Different behaviors have appeared depending on the boundary conditions of the structure. While for hiperestatic structures the sequence of the upper and lower bounds has the expected behavior, for the case of isostatic structures, it has been found that the lower bound remains constant as the mesh is refined.

In future papers we will try to find out more about the behavior of the lower bound in the case of isostatic structures. It can be interesting to prove that the lower bound remains constant in this case.

It is important, once again, to focus on the importance of the consideration a-priori of a reference mesh. The exposed method supposes an initial very fine mesh or reference mesh. This is the mesh towards the bounds are converging. It is essential to be consistent with this mesh. This means that in each refinement step the number of used elements to find the lower bound cannot be arbitrary. This is that the number of element in which each element is divided when finding the lower bound is conditioned to the reference mesh mentioned before. The way both meshes are linked is that if we put together all the meshes of all the elements, when finding the lower bound, it give us the reference mesh supposed before. This fact is very important, otherwise, we could have found behaviors like the one shown in figure(7.1). You can see that the lower bound is decreasing when improving the mesh. This happens because it is not converging towards a fixed solution.

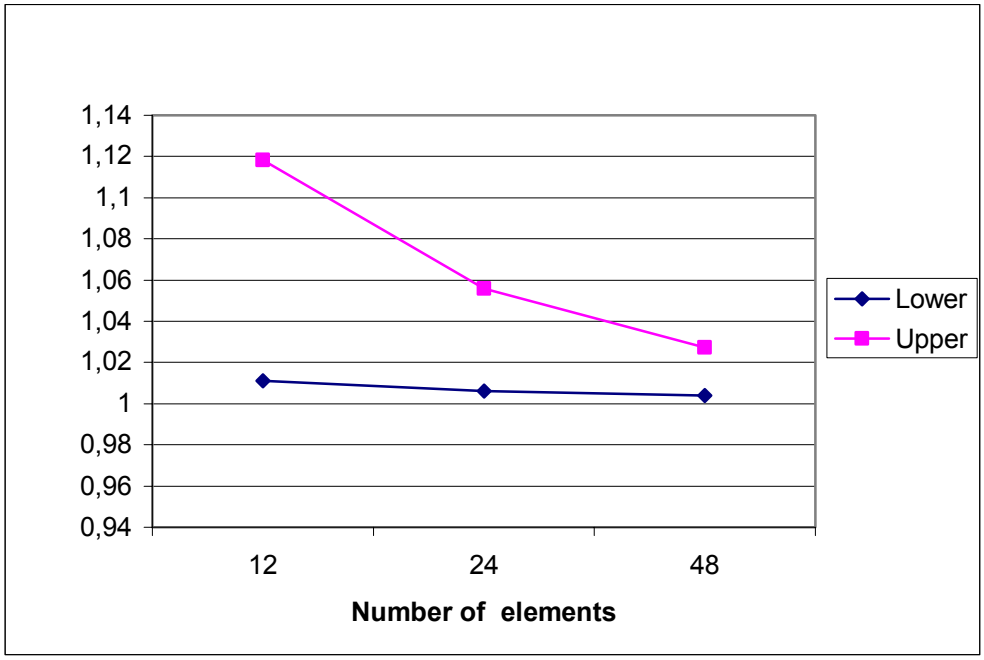

Figure7.1 Upper bound and Lower bound convergence

The structure of the implemented program makes easy to ad improvements to it. For example, in the future we will introduce other kind of loads. An important improvement of the program could be to adapt it for the case of inclined boundary conditions. This is when the boundary conditions do not coincide with the global axis. It just have to be changed the global degrees of freedom in the system of equations for their local ones. It can be done by multiplying the rows and columns of the global stiffness matrix affected by the right terms of changing of axis.

In summary, a method that allow us to find a sequence of upper and lower bounds to a specific collapse load of a structure. We have focused in the case of proportional loading only. To consider that loads can vary independently one from the other escapes from the aim of this work. The method has been tested for planar frames considering different contributions of the internal forces. The application of the method to more complex structures as shells is the aim of more advanced papers.

REFERENCES

Milan J., Zdenek P. (2001), *Inelastic analysis of structures*, published by J. Wiley and Sons.

Lynn S. Beedle (1958), *Plastic design of steel frames*, published by Chapman and Hall.

J Chakrabarty (1987), *Theory of plasticity*, published by McGraw-Hill.

Lubliner Jacob (1990), *Plastic Theory*, published by Macmillan.

James McCulloch (2002), *Limit state truss and beam analysis,* published by Yr Adran Peirianneg Sifil.

O.C. Zienkiewicz (1967), *The finite element method*, published by McGraw-Hill

Z. Waszczyszyn, C Cichon, M. Radwanska (1994), *Stability of structures by finite element methods*, published by Elsevier.

J. Bonet, A. Huerta, J. Peraire (2002), *The efficient computation of bounds for functionals of finite element solutions in large strain elasticity*, published by Elsevier.

M. Ainsworth, J.T. Oden (2000), *A Posteriori Error Estimatin in Finite Element Analysis*, published by Wiley-Interscience.

P. Ladeveze, D. Leguillon (1983), *Error estimate procedure in the finite element method and applications,* SIAM J. Number. Anal. 20

A.R.S. Ponter, K.F. Carter (1995), *Limit state solutions, based upon linear elastic solutions with a spatially varying elastic modulus*, published by Elsevier.

A.R.S Ponter, Paolo Fuschi and Markus Elgenlhardt (2000), *Limit analysis for a general class of yield conditions*, published by Elsevier.

A.R.S. Ponter and S. Karadeniz (1980), *A linear programming upper bound approach to the shakedown limit of thin shells subjected to variable thermal loading*, J. Strain Anal. 19.

K.F.Carter and A.R.S. Ponter (1990), *Interaction diagrams and design rules for axisymetric thin shells subjected to cyclic thermal loading*, Final report: UKAEA Contract IR 55721.

D. Mackenzie, C. Nadarajah, J. Shi and J.T. Boyle (1993), *Simple bounds on limit loads by elastic finite element finite analysis*, ASME J. Press Ves. Tech. 115.

J. Shi, D. Mackenzie, and J.T.Boyle (1993), *A method of estimating limit loads by iterative elastic analysis*, Int. J. Pres. Ves. Pipin 53.